activator recruitment; i.e., the ATPase activity of PA700 drives a stable association of a transactivator with the SAGA histone acetyltransferase complex.[131] PA700 also acts nonproteolytically in nuclear excision repair (NER).[132),133] Chromatin remodeling is another nonproteolytic role of PA700, with implications for both transcription and DNA repair.[131] In addition, a proteasome-derived ATPase activity mediates relocalization of the substrates of endoplasmic reticulum-associated degradation (ERAD), a function that is primarily attributed to the AAA-ATPase p97/Cdc48.[134] ERAD eliminates aberrant proteins from the ER by localizing them to the cytoplasm where they are tagged by ubiquitin and degraded by the proteasome.

As described before, PI31 and PR39 are naturally occurring proteasome inhibitors, but their physiological functions are unclear. On the other hand, membrane-permeable synthetic inhibitors have been devised; e.g., various substrate-related peptidyl aldehydes have been designed as potent inhibitors of proteasomes, such as MG-132 (*N*-carbobenzoxy-Leu-Leu-leucinal) and PSI (*N*-carbobenzoxy-L-gamma-t-butyl-L-glutamyl-L-alanyl-L-leucinal), and the non-aldehyde peptidyl inhibitor Z-L_3VS (carboxybenzyl-leucyl-leucyl-leucine vinyl sulfone), which are often used in *in vitro* and *in vivo* experiments.[135),136] However, caution must be exercised in their use for inferring proteasome functions, because they inhibit not only proteasomes but also cysteine proteases such as calpains and lysosomal cathepsins.[135] In contrast to these compounds, microbial metabolites, lactacystin and epoxomicin, were found to be selective proteasome inhibitors that do not affect other proteases examined so far.[137),138] Of particular interest is bortezomib (also known as velcade or PS-341). Bortezomib as first-in-class proteasome inhibitor has proven to be highly effective in some hematological malignancies, and in fact it has been granted approval by the FDA for relapsed multiple myeloma and non-Hodgkin lymphoma (NHL) and has been used clinically in over 85 countries worldwide so far.[139] Moreover, preclinical studies demonstrate that proteasome inhibition potentiates the activity of other cancer therapeutics, and particularly, the combination of proteasome inhibition with novel targeted therapies is an emerging field in oncology.[140] Furthermore, Salinosporamide A (also called NPI-0052),[141] recently identified from the marine bacterium *Salinispora tropica*, is a potent inhibitor of 20S proteasome and exhibits therapeutic potential against a wide variety of tumors. In addition, many other proteasome inhibitors are being assessed clinically for therapeutic use.[142] Thus, proteasome inhibitors provide a powerful new tool as fashionable drugs against cancer and other diseases including inflammations.

Finally, it should be emphasized that studies of the proteasome continue to provide significant insights in the physiologic roles of these complexes. Many questions, however, remain to be uncovered.

Acknowledgements

This work was supported by grants from the Ministry of Education, Culture, Sports, Science and Technology (MEXT) of Japan; the Target Protein Project of MEXT; and Health and Labor Science Research Grants.

References

1) Hershko, A. and Ciechanover, A. (1998) The ubiquitin system. Annu. Rev. Biochem. **67**, 425–479.
2) Ravid, T. and Hochstrasser, M. (2008) Diversity of degradation signals in the ubiquitin-proteasome system. Nat. Rev. Mol. Cell Biol. **9**, 679–690.
3) Ventii, K. H. and Wilkinson, K. D. (2008) Protein partners of deubiquitinating enzymes. Biochem. J. **414**, 161–175.
4) Varshavsky, A. (2005) Regulated protein degradation. Trends Biochem. Sci. **30**, 283–286.
5) Ciechanover, A. (2006) The ubiquitin proteolytic system: from a vague idea, through basic mechanisms, and onto human diseases and drug targeting. Neurology **66**, S7-19.
6) Tai, H. C. and Schuman, E. M. (2008) Ubiquitin, the proteasome and protein degradation in neuronal function and dysfunction. Nat. Rev. Neurosci. **9**, 826–838.
7) Coux, O., Tanaka, K. and Goldberg, A. L. (1996) Structure and functions of the 20S and 26S proteasomes. Annu. Rev. Biochem. **65**, 801–847.
8) Baumeister, W., Walz, J., Zuhl, F. and Seemuller, E. (1998) The proteasome: paradigm of a self-compartmentalizing protease. Cell **92**, 367–380.
9) Demartino, G. N. and Gillette, T. G. (2007) Proteasomes: machines for all reasons. Cell **129**, 659–662.
10) Yoshimura, T., Kameyama, K., Takagi, T., Ikai, A., Tokunaga, F., Koide, T., Tanahashi, N., Tamura, T., Tanaka, K., Cejka, Z. *et al.* (1993) Molecular characterization of the '26S' proteasome complex from rat liver. J. Struct. Biol. **111**, 200–211.

11) Maupin-Furlow, J. A., Humbard, M. A., Kirkland, P. A., Li, W., Reuter, C. J., Wright, A. J. and Zhou, G. (2006) Proteasomes from structure to function: perspectives from Archaea. Curr. Top. Dev. Biol. **75**, 125–169.
12) Groll, M., Ditzel, L., Lowe, J., Stock, D., Bochtler, M., Bartunik, H. D. and Huber, R. (1997) Structure of 20S proteasome from yeast at 2.4 A resolution. Nature **386**, 463–471.
13) Unno, M., Mizushima, T., Morimoto, Y., Tomisugi, Y., Tanaka, K., Yasuoka, N. and Tsukihara, T. (2002) The structure of the mammalian 20S proteasome at 2.75 A resolution. Structure **10**, 609–618.
14) Bochtler, M., Ditzel, L., Groll, M., Hartmann, C. and Huber, R. (1999) The proteasome. Annu. Rev. Biophys. Biomol. Struct. **28**, 295–317.
15) Kloetzel, P. M. and Ossendorp, F. (2004) Proteasome and peptidase function in MHC-class-I-mediated antigen presentation. Curr. Opin. Immunol. **16**, 76–81.
16) Liu, C. W., Corboy, M. J., DeMartino, G. N. and Thomas, P. J. (2003) Endopoteolytic activity of the proteasome. Science **299**, 408–411.
17) Jung, T. and Grune, T. (2008) The proteasome and its role in the degradation of oxidized proteins. IUBMB Life **60**, 743–752.
18) Glickman, M. H., Rubin, D. M., Fried, V. A. and Finley, D. (1998) The regulatory particle of the Saccharomyces cerevisiae proteasome. Mol. Cell Biol. **18**, 3149–3162.
19) Hanna, J. and Finley, D. (2007) A proteasome for all occasions. FEBS Lett. **581**, 2854–2861.
20) Verma, R., Aravind, L., Oania, R., McDonald, W. H., Yates, J. R. 3rd, Koonin, E. V. and Deshaies, R. J. (2002) Role of Rpn11 metalloprotease in deubiquitination and degradation by the 26S proteasome. Science **298**, 611–615.
21) Hu, M., Li, P., Song, L., Jeffrey, P. D., Chenova, T. A., Wilkinson, K. D., Cohen, R. E. and Shi, Y. (2005) Structure and mechanisms of the proteasome-associated deubiquitinating enzyme USP14. EMBO J. **24**, 3747–3756.
22) Hamazaki, J., Iemura, S., Natsume, T., Yashiroda, H., Tanaka, K. and Murata, S. (2006) A novel proteasome interacting protein recruits the deubiquitinating enzyme UCH37 to 26S proteasomes. EMBO J. **25**, 4524–4536.
23) Yao, T., Song, L., Xu, W., DeMartino, G. N., Florens, L., Swanson, S. K., Washburn, M. P., Conaway, R. C., Conaway, J. W. and Cohen, R. E. (2006) Proteasome recruitment and activation of the Uch37 deubiquitinating enzyme by Adrm1. Nat. Cell Biol. **8**, 994–1002.
24) Hanna, J., Meides, A., Zhang, D. P. and Finley, D. (2007) A ubiquitin stress response induces altered proteasome composition. Cell **129**, 747–759.
25) Rosenzweig, R., Osmulski, P. A., Gaczynska, M. and Glickman, M. H. (2008) The central unit within the 19S regulatory particle of the proteasome. Nat. Struct. Mol. Biol. **15**, 573–580.
26) Deveraux, Q., van Nocker, S., Mahaffey, D., Vierstra, R. and Rechsteiner, M. (1995) Inhibition of ubiquitin-mediated proteolysis by the Arabidopsis 26 S protease subunit S5a. J. Biol. Chem. **270**, 29660–29663.
27) Schreiner, P., Chen, X., Husnjak, K., Randles, L., Zhang, N., Elsasser, S., Finley, D., Dikic, I., Walters, K. J. and Groll, M. (2008) Ubiquitin docking at the proteasome through a novel pleckstrin-homology domain interaction. Nature **453**, 548–552.
28) Husnjak, K., Elsasser, S., Zhang, N., Chen, X., Randles, L., Shi, Y., Hofmann, K., Walters, K. J., Finley, D. and Dikic, I. (2008) Proteasome subunit Rpn13 is a novel ubiquitin receptor. Nature **453**, 481–488.
29) Saeki, Y. and Tanaka, K. (2008) Cell biology: two hands for degradation. Nature **453**, 460–461.
30) Lam, Y. A., Lawson, T. G., Velayutham, M., Zweier, J. L. and Pickart, C. M. (2002) A proteasomal ATPase subunit recognizes the polyubiquitin degradation signal. Nature **416**, 763–767.
31) Kang, Y., Vossler, R. A., Diaz-Martinez, L. A., Winter, N. S., Clarke, D. J. and Walters, K. J. (2006) UBL/UBA ubiquitin receptor proteins bind a common tetraubiquitin chain. J. Mol. Biol. **356**, 1027–1035.
32) Madura, K. (2004) Rad23 and Rpn10: perennial wallflowers join the melee. Trends Biochem. Sci. **29**, 637–640.
33) Hartmann-Petersen, R. and Gordon, C. (2004) Integral UBL domain proteins: a family of proteasome interacting proteins. Semin. Cell Dev. Biol. **15**, 247–259.
34) Moscat, J., Diaz-Meco, M. T. and Wooten, M. W. (2007) Signal integration and diversification through the p62 scaffold protein. Trends Biochem. Sci. **32**, 95–100.
35) Elsasser, S. and Finley, D. (2005) Delivery of ubiquitinated substrates to protein-unfolding machines. Nat. Cell Biol. **7**, 742–749.
36) Komatsu, M., Waguri, S., Koike, M., Sou, Y. S., Ueno, T., Hara, T., Mizushima, N., Iwata, J., Ezaki, J., Murata, S. *et al.* (2007) Homeostatic levels of p62 control cytoplasmic inclusion body formation in autophagy-deficient mice. Cell **131**, 1149–1163.
37) Ichimura, Y., Kumanomidou, T., Sou, Y. S., Mizushima, T., Ezaki, J., Ueno, T., Kominami, E., Yamane, T., Tanaka, K. and Komatsu, M. (2008) Structural basis for sorting mechanism of p62 in selective autophagy. J. Biol. Chem. **283**, 22847–22857.
38) Elsasser, S., Gali, R. R., Schwickart, M., Larsen, C. N., Leggett, D. S., Muller, B., Feng, M. T., Tubing, F., Dittmar, G. A. and Finley, D. (2002) Proteasome subunit Rpn1 binds ubiquitin-like protein domains. Nat. Cell Biol. **4**, 725–730.
39) Rechsteiner, M., Realini, C. and Ustrell, V. (2000) The proteasome activator 11 S REG (PA28) and

class I antigen presentation. Biochem. J. **345**, 1–15.
40) Forster, A., Masters, E. I., Whitby, F. G., Robinson, H. and Hill, C. P. (2005) The 1.9 A structure of a proteasome-11S activator complex and implications for proteasome-PAN/PA700 interactions. Mol. Cell **18**, 589–599.
41) Smith, D. M., Chang, S. C., Park, S., Finley, D., Cheng, Y. and Goldberg, A. L. (2007) Docking of the proteasomal ATPases' carboxyl termini in the 20S proteasome's alpha ring opens the gate for substrate entry. Mol. Cell **27**, 731–744.
42) Rabl, J., Smith, D. M., Yu, Y., Chang, S. C., Goldberg, A. L. and Cheng, Y. (2008) Mechanism of gate opening in the 20S proteasome by the proteasomal ATPases. Mol. Cell **30**, 360–368.
43) Saeki, Y. and Tanaka, K. (2007) Unlocking the proteasome door. Mol. Cell **27**, 865–867.
44) Liu, C. W., Li, X., Thompson, D., Wooding, K., Chang, T. L., Tang, Z., Yu, H., Thomas, P. J. and DeMartino, G. N. (2006) ATP binding and ATP hydrolysis play distinct roles in the function of 26S proteasome. Mol. Cell **24**, 39–50.
45) Braun, B. C., Glickman, M., Kraft, R., Dahlmann, B., Kloetzel, P. M., Finley, D. and Schmidt, M. (1999) The base of the proteasome regulatory particle exhibits chaperone-like activity. Nat. Cell Biol. **1**, 221–226.
46) Tanahashi, N., Yokota, K., Ahn, J. Y., Chung, C. H., Fujiwara, T., Takahashi, E., DeMartino, G. N., Slaughter, C. A., Toyonaga, T., Yamamura, K., Shimbara, N. and Tanaka, K. (1997) Molecular properties of the proteasome activator PA28 family proteins and gamma-interferon regulation. Genes Cells **2**, 195–211.
47) Wojcik, C., Tanaka, K., Paweletz, N., Naab, U. and Wilk, S. (1998) Proteasome activator (PA28) subunits, alpha, beta and gamma (Ki antigen) in NT2 neuronal precursor cells and HeLa S3 cells. Eur. J. Cell Biol. **77**, 151–160.
48) Whitby, F. G., Masters, E. I., Kramer, L., Knowlton, J. R., Yao, Y., Wang, C. C. and Hill, C. P. (2000) Structural basis for the activation of 20S proteasomes by 11S regulators. Nature **408**, 115–120.
49) Murata, S., Udono, H., Tanahashi, N., Hamada, N., Watanabe, K., Adachi, K., Yamano, T., Yui, K., Kobayashi, N., Kasahara, M. *et al.* (2001) Immunoproteasome assembly and antigen presentation in mice lacking both PA28alpha and PA28beta. EMBO J. **20**, 5898–5907.
50) Tanaka, K. and Kasahara, M. (1998) The MHC class I ligand-generating system: roles of immunoproteasomes and the interferon-gamma-inducible proteasome activator PA28. Immunol. Rev. **163**, 161–176.
51) Kloetzel, P. M. (2001) Antigen processing by the proteasome. Nat. Rev. Mol. Cell Biol. **2**, 179–187.
52) Rock, K. L., York, I. A., Saric, T. and Goldberg, A. L. (2002) Protein degradation and the generation of MHC class I-presented peptides. Adv. Immunol. **80**, 1–70.
53) Murata, S., Kawahara, H., Tohma, S., Yamamoto, K., Kasahara, M., Nabeshima, Y., Tanaka, K. and Chiba, T. (1999) Growth retardation in mice lacking the proteasome activator PA28-gamma. J. Biol. Chem. **274**, 38211–38215.
54) Zhang, Z. and Zhang, R. (2008) Proteasome activator PA28 gamma regulates p53 by enhancing its MDM2-mediated degradation. EMBO J. **27**, 852–864.
55) Li, X., Lonard, D. M., Jung, S. Y., Malovannaya, A., Feng, Q., Qin, J., Tsai, S. Y., Tsai, M. J. and O'Malley, B. W. (2006) The SRC-3/AIB1 coactivator is degraded in a ubiquitin- and ATP-independent manner by the REGgamma proteasome. Cell **124**, 381–392.
56) Li, X., Amazit, L., Long, W., Lonard, D. M., Monaco, J. J. and O'Malley, B. W. (2007) Ubiquitin- and ATP-independent proteolytic turnover of p21 by the REGgamma-proteasome pathway. Mol. Cell **26**, 831–842.
57) Chen, X., Barton, L. F., Chi, Y., Clurman, B. E. and Roberts, J. M. (2007) Ubiquitin-independent degradation of cell-cycle inhibitors by the REGgamma proteasome. Mol. Cell **26**, 843–852.
58) Zannini, L., Lecis, D., Buscemi, G., Carlessi, L., Gasparini, P., Fontanella, E., Lisanti, S., Barton, L. and Delia, D. (2008) REGgamma proteasome activator is involved in the maintenance of chromosomal stability. Cell Cycle **7**, 504–512.
59) Mao, I., Liu, J., Li, X. and Luo, H. (2008) REGgamma, a proteasome activator and beyond. Cell Mol. Life Sci. (in press).
60) Moriishi, K., Mochizuki, R., Moriya, K., Miyamoto, H., Mori, Y., Abe, T., Murata, S., Tanaka, K., Miyamura, T., Suzuki, T. *et al.* (2007) Critical role of PA28gamma in hepatitis C virus-associated steatogenesis and hepatocarcinogenesis. Proc. Natl. Acad. Sci. USA **104**, 1661–1666.
61) Tanahashi, N., Murakami, Y., Minami, Y., Shimbara, N., Hendil, K. B. and Tanaka, K. (2000) Hybrid proteasomes. Induction by interferon-gamma and contribution to ATP-dependent proteolysis. J. Biol. Chem. **275**, 14336–14345.
62) Cascio, P., Call, M., Petre, B. M., Walz, T. and Goldberg, A. L. (2002) Properties of the hybrid form of the 26S proteasome containing both 19S and PA28 complexes. EMBO J. **21**, 2636–2645.
63) Kopp, F., Dahlmann, B. and Kuehn, L. (2001) Reconstitution of hybrid proteasomes from purified PA700-20 S complexes and PA28alphabeta activator: ultrastructure and peptidase activities. J. Mol. Biol. **313**, 465–471.
64) Murakami, Y., Matsufuji, S., Kameji, T., Hayashi, S., Igarashi, K., Tamura, T., Tanaka, K. and Ichihara, A. (1992) Ornithine decarboxylase is

degraded by the 26S proteasome without ubiquitination. Nature **360**, 597–599.
65) Ustrell, V., Hoffman, L., Pratt, G. and Rechsteiner, M. (2002) PA200, a nuclear proteasome activator involved in DNA repair. EMBO J. **21**, 3516–3525.
66) Schmidt, M., Haas, W., Crosas, B., Santamaria, P. G., Gygi, S. P., Walz, T. and Finley, D. (2005) The HEAT repeat protein Blm10 regulates the yeast proteasome by capping the core particle. Nat. Struct. Mol. Biol. **12**, 294–303.
67) Fehlker, M., Wendler, P., Lehmann, A. and Enenkel, C. (2003) Blm3 is part of nascent proteasomes and is involved in a late stage of nuclear proteasome assembly. EMBO Rep. **4**, 959–963.
68) Marques, A. J., Glanemann, C., Ramos, P. C. and Dohmen, R. J. (2007) The C-terminal extension of the beta7 subunit and activator complexes stabilize nascent 20 S proteasomes and promote their maturation. J. Biol. Chem. **282**, 34869–34876.
69) Ortega, J., Heymann, J. B., Kajava, A. V., Ustrell, V., Rechsteiner, M. and Steven, A. C. (2005) The axial channel of the 20S proteasome opens upon binding of the PA200 activator. J. Mol. Biol. **346**, 1221–1227.
70) Iwanczyk, J., Sadre-Bazzaz, K., Ferrell, K., Kondrashkina, E., Formosa, T., Hill, C. P. and Ortega, J. (2006) Structure of the Blm10-20 S proteasome complex by cryo-electron microscopy. Insights into the mechanism of activation of mature yeast proteasomes. J. Mol. Biol. **363**, 648–659.
71) Lehmann, A., Jechow, K. and Enenkel, C. (2008) Blm10 binds to pre-activated proteasome core particles with open gate conformation. EMBO Rep. (in press).
72) Blickwedehl, J., Agarwal, M., Seong, C., Pandita, R. K., Melendy, T., Sung, P., Pandita, T. K. and Bangia, N. (2008) Role for proteasome activator PA200 and postglutamyl proteasome activity in genomic stability. Proc. Natl. Acad. Sci. USA **105**, 16165–16170.
73) Khor, B., Bredemeyer, A. L., Huang, C. Y., Turnbull, I. R., Evans, R., Maggi, L. B. Jr., White, J. M., Walker, L. M., Carnes, K., Hess, R. A. and Sleckman, B. P. (2006) Proteasome activator PA200 is required for normal spermatogenesis. Mol. Cell Biol. **26**, 2999–3007.
74) McCutchen-Maloney, S. L., Matsuda, K., Shimbara, N., Binns, D. D., Tanaka, K., Slaughter, C. A. and DeMartino, G. N. (2000) cDNA cloning, expression, and functional characterization of PI31, a proline-rich inhibitor of the proteasome. J. Biol. Chem. **275**, 18557–18565.
75) Zaiss, D. M., Standera, S., Kloetzel, P. M. and Sijts, A. J. (2002) PI31 is a modulator of proteasome formation and antigen processing. Proc. Natl. Acad. Sci. USA **99**, 14344–14349.
76) Kirk, R., Laman, H., Knowles, P. P., Murray-Rust, J., Lomonosov, M., Mezianeel, K. and McDonald, N. Q. (2008) Structure of a conserved dimerization domain within the F-box protein Fbxo7 and the PI31 proteasome inhibitor. J. Biol. Chem. **283**, 22325–22335.
77) Rechsteiner, M. and Hill, C. P. (2005) Bilizing the proteolytic machine: cell biological roles of proteasome activators and inhibitors. Trends Cell Biol. **15**, 27–33.
78) Anbanandam, A., Albarado, D. C., Tirziu, D. C., Simons, M. and Veeraraghavan, S. (2008) Molecular basis for proline- and arginine-rich peptide inhibition of proteasome. J. Mol. Biol. **384**, 219–227.
79) Smalle, J. and Vierstra, R. D. (2004) The ubiquitin 26S proteasome proteolytic pathway. Annu. Rev. Plant Biol. **55**, 555–590.
80) Belote, J. M. and Zhong, L. (2005) Proteasome gene duplications in mammals, flies and plants. Recent Res. Devel. Gene & Genomes **1**, 107–129.
81) Fu, H., Doelling, J. H., Arendt, C. S., Hochstrasser, M. and Vierstra, R. D. (1998) Molecular organization of the 20S proteasome gene family from Arabidopsis thaliana. Genetics **149**, 677–692.
82) Fehling, H. J., Swat, W., Laplace, C., Kuhn, R., Rajewsky, K., Muller, U. and von Boehmer, H. (1994) MHC class I expression in mice lacking the proteasome subunit LMP-7. Science **265**, 1234–1237.
83) van Kaer, L., Ashton-Rickardt, P. G., Eichelberger, M., Gaczynska, M., Nagashima, K., Rock, K. L., Goldberg, A. L., Doherty, P. C. and Tonegawa, S. (1994) Altered peptidase and viral-specific T cell response in LMP2 mutant mice. Immunity **1**, 533–541.
84) Barton, L. F., Runnels, H. A., Schell, T. D., Cho, Y., Gibbons, R., Tevethia, S. S., Deepe, G. S. Jr. and Monaco, J. J. (2004) Immune defects in 28-kDa proteasome activator gamma-deficient mice. J. Immunol. **172**, 3948–3954.
85) Kasahara, M., Hayashi, M., Tanaka, K., Inoko, H., Sugaya, K., Ikemura, T. and Ishibashi, T. (1996) Chromosomal localization of the proteasome Z subunit gene reveals an ancient chromosomal duplication involving the major histocompatibility complex. Proc. Natl. Acad. Sci. USA **93**, 9096–9101.
86) Murata, S., Sasaki, K., Kishimoto, T., Niwa, S., Hayashi, H., Takahama, Y. and Tanaka, K. (2007) Regulation of $CD8^+$ T cell development by thymus-specific proteasomes. Science **316**, 1349–1353.
87) Murata, S., Takahama, Y. and Tanaka, K. (2008) Thymoproteasome: probable role in generating positively selecting peptides. Curr. Opin. Immunol. **20**, 192–196.
88) Takahama, Y., Tanaka, K. and Murata, S. (2008) Modest cortex and promiscuous medulla for thymic repertoire formation. Trends Immunol. **29**, 251–255.
89) Nitta, T., Murata, S., Ueno, T., Tanaka, K. and

Takahama, Y. (2008) Thymic environments of T-cell repertoire formation. Adv. Immunol. (in press).
90) Zhong, L. and Belote, J. M. (2007) The testis-specific proteasome subunit Prosalpha6 T of D. melanogaster is required for individualization and nuclear maturation during spermatogenesis. Development **134**, 3517–3525.
91) Kawahara, H., Kasahara, M., Nishiyama, A., Ohsumi, K., Goto, T., Kishimoto, T., Saeki, Y., Yokosawa, H., Shimbara, N., Murata, S. *et al.* (2000) Developmentally regulated, alternative splicing of the Rpn10 gene generates multiple forms of 26S proteasomes. EMBO J. **19**, 4144–4153.
92) Hamazaki, J., Sasaki, K., Kawahara, H., Hisanaga, S., Tanaka, K. and Murata, S. (2007) Rpn10-mediated degradation of ubiquitinated proteins is essential for mouse development. Mol. Cell Biol. **27**, 6629–6638.
93) Stanhill, A., Haynes, C. M., Zhang, Y., Min, G., Steele, M. C., Kalinina, J., Martinez, E., Pickart, C. M., Kong, X. P. and Ron, D. (2006) An arsenite-inducible 19S regulatory particle-associated protein adapts proteasomes to proteotoxicity. Mol. Cell **23**, 875–885.
94) Yun, C., Stanhill, A., Yang, Y., Zhang, Y., Haynes, C. M., Xu, C. F., Neubert, T. A., Mor, A., Philips, M. R. and Ron, D. (2008) Proteasomal adaptation to environmental stress links resistance to proteotoxicity with longevity in Caenorhabditis elegans. Proc. Natl. Acad. Sci. USA **105**, 7094–7099.
95) Ellis, R. J. (2006) Molecular chaperones: assisting assembly in addition to folding. Trends Biochem. Sci. **31**, 395–401.
96) Kusmierczyk, A. R. and Hochstrasser, M. (2008) Some assembly required: dedicated chaperones in eukaryotic proteasome biogenesis. Biol. Chem. **389**, 1143–1151.
97) Ramos, P. C. and Dohmen, R. J. (2008) PACemakers of proteasome core particle assembly. Structure **16**, 1296–304.
98) Murata, S., Yashiroda, H. and Tanaka, K. (2009) Molecular mechanisms of proteasome assembly. Nat. Rev. Mol. Cell Biol. (in press).
99) Rosenzweig, R. and Glickman, M. H. (2008) Chaperone-driven proteasome assembly. Biochem. Soc. Trans. **36**, 807–812.
100) Hirano, Y., Hendil, K. B., Yashiroda, H., Iemura, S., Nagane, R., Hioki, Y., Natsume, T., Tanaka, K. and Murata, S. (2005) A heterodimeric complex that promotes the assembly of mammalian 20S proteasomes. Nature **437**, 1381–1385.
101) Li, X., Kusmierczyk, A. R., Wong, P., Emili, A. and Hochstrasser, M. (2007) Beta-Subunit appendages promote 20S proteasome assembly by overcoming an Ump1-dependent checkpoint. EMBO J. **26**, 2339–2349.
102) Hirano, Y., Hayashi, H., Iemura, S., Hendil, K. B., Niwa, S., Kishimoto, T., Kasahara, M., Natsume, T., Tanaka, K. and Murata, S. (2006) Cooperation of multiple chaperones required for the assembly of mammalian 20S proteasomes. Mol. Cell **24**, 977–984.
103) Le Tallec, B., Barrault, M. B., Courbeyrette, R., Guerois, R., Marsolier-Kergoat, M. C. and Peyroche, A. (2007) 20S proteasome assembly is orchestrated by two distinct pairs of chaperones in yeast and in mammals. Mol. Cell **27**, 660–674.
104) Yashiroda, H., Mizushima, T., Okamoto, K., Kameyama, T., Hayashi, H., Kishimoto, T., Niwa, S., Kasahara, M., Kurimoto, E., Sakata, E. *et al.* (2008) Crystal structure of a chaperone complex that contributes to the assembly of yeast 20S proteasomes. Nat. Struct. Mol. Biol. **15**, 228–236.
105) Kusmierczyk, A. R., Kunjappu, M. J., Funakoshi, M. and Hochstrasser, M. (2008) A multimeric assembly factor controls the formation of alternative 20S proteasomes. Nat. Struct. Mol. Biol. **15**, 237–244.
106) Hoyt, M. A., McDonough, S., Pimpl, S. A., Scheel, H., Hofmann, K. and Coffino, P. (2008) A genetic screen for Saccharomyces cerevisiae mutants affecting proteasome function, using a ubiquitin-independent substrate. Yeast **25**, 199–217.
107) Shinde, U. and Inouye, M. (2000) Intramolecular chaperones: polypeptide extensions that modulate protein folding. Semin Cell Dev. Biol. **11**, 35–44.
108) De, M., Jayarapu, K., Elenich, L., Monaco, J. J., Colbert, R. A. and Griffin, T. A. (2003) Beta 2 subunit propeptides influence cooperative proteasome assembly. J. Biol. Chem. **278**, 6153–6159.
109) Chen, P. and Hochstrasser, M. (1996) Autocatalytic subunit processing couples active site formation in the 20S proteasome to completion of assembly. Cell **86**, 961–972.
110) Hirano, Y., Kaneko, T., Okamoto, K., Bai, M., Yashiroda, H., Furuyama, K., Kato, K., Tanaka, K. and Murata, S. (2008) Dissecting beta-ring assembly pathway of the mammalian 20S proteasome. EMBO J. **27**, 2204–2213.
111) Ramos, P. C., Hockendorff, J., Johnson, E. S., Varshavsky, A. and Dohmen, R. J. (1998) Ump1p is required for proper maturation of the 20S proteasome and becomes its substrate upon completion of the assembly. Cell **92**, 489–499.
112) Witt, E., Zantopf, D., Schmidt, M., Kraft, R., Kloetzel, P. M. and Kruger, E. (2000) Characterisation of the newly identified human Ump1 homologue POMP and analysis of LMP7(beta 5i) incorporation into 20 S proteasomes. J. Mol. Biol. **301**, 1–9.
113) Griffin, T. A., Slack, J. P., McCluskey, T. S., Monaco, J. J. and Colbert, R. A. (2000) Identification of proteassemblin, a mammalian homologue of the yeast protein, Ump1p, that is

required for normal proteasome assembly. Mol. Cell Biol. Res. Commun. **3**, 212–217.
114) Griffin, T. A., Nandi, D., Cruz, M., Fehling, H. J., Kaer, L. V., Monaco, J. J. and Colbert, R. A. (1998) Immunoproteasome assembly: cooperative incorporation of interferon gamma (IFN-gamma)-inducible subunits. J. Exp. Med. **187**, 97–104.
115) Kingsbury, D. J., Griffin, T. A. and Colbert, R. A. (2000) Novel propeptide function in 20 S proteasome assembly influences beta subunit composition. J. Biol. Chem. **275**, 24156–24162.
116) Heink, S., Ludwig, D., Kloetzel, P. M. and Kruger, E. (2005) IFN-gamma-induced immune adaptation of the proteasome system is an accelerated and transient response. Proc. Natl. Acad. Sci. USA **102**, 9241–9246.
117) Isono, E., Nishihara, K., Saeki, Y., Yashiroda, H., Kamata, N., Ge, L., Ueda, T., Kikuchi, Y., Tanaka, K., Nakano, A. and Toh-e, A. (2007) The assembly pathway of the 19S regulatory particle of the yeast 26S proteasome. Mol. Biol. Cell **18**, 569–580.
118) Isono, E., Saito, N., Kamata, N., Saeki, Y. and Toh, E. A. (2005) Functional analysis of Rpn6p, a lid component of the 26 S proteasome, using temperature-sensitive rpn6 mutants of the yeast Saccharomyces cerevisiae. J. Biol. Chem. **280**, 6537–6547.
119) Imai, J., Maruya, M., Yashiroda, H., Yahara, I. and Tanaka, K. (2003) The molecular chaperone Hsp90 plays a role in the assembly and maintenance of the 26S proteasome. EMBO J. **22**, 3557–3567.
120) Kleijnen, M. F., Roelofs, J., Park, S., Hathaway, N. A., Glickman, M., King, R. W. and Finley, D. (2007) Stability of the proteasome can be regulated allosterically through engagement of its proteolytic active sites. Nat. Struct. Mol. Biol. **14**, 1180–1188.
121) Babbitt, S. E., Kiss, A., Deffenbaugh, A. E., Chang, Y. H., Bailly, E., Erdjument-Bromage, H., Tempst, P., Buranda, T., Sklar, L. A., Baumler, J. *et al.* (2005) ATP hydrolysis-dependent disassembly of the 26S proteasome is part of the catalytic cycle. Cell **121**, 553–565.
122) Kriegenburg, F., Seeger, M., Saeki, Y., Tanaka, K., Lauridsen, A. M. B., Hartmann-Petersen, R. and Hendil, K. B. (2008) Mammalian 26S proteasomes remain intact during protein degradation. Cell **135**, 355–365.
123) Verma, R., Chen, S., Feldman, R., Schieltz, D., Yates, J., Dohmen, J. and Deshaies, R. J. (2000) Proteasomal proteomics: identification of nucleotide-sensitive proteasome-interacting proteins by mass spectrometric analysis of affinity-purified proteasomes. Mol. Biol. Cell **11**, 3425–3439.
124) Guerrero, C., Tagwerker, C., Kaiser, P. and Huang, L. (2006) An integrated mass spectrometry-based proteomic approach: quantitative analysis of tandem affinity-purified *in vivo* cross-linked protein complexes (QTAX) to decipher the 26 S proteasome-interacting network. Mol. Cell Proteomics **5**, 366–378.
125) Wang, X., Chen, C. F., Baker, P. R., Chen, P. L., Kaiser, P. and Huang, L. (2007) Mass spectrometric characterization of the affinity-purified human 26S proteasome complex. Biochemistry **46**, 3553–65.
126) Leggett, D. S., Hanna, J., Borodovsky, A., Crosas, B., Schmidt, M., Baker, R. T., Walz, T., Ploegh, H. and Finley, D. (2002) Multiple associated proteins regulate proteasome structure and function. Mol. Cell **10**, 495–507.
127) Gorbea, C., Goellner, G. M., Teter, K., Holmes, R. K. and Rechsteiner, M. (2004) Characterization of mammalian Ecm29, a 26 S proteasome-associated protein that localizes to the nucleus and membrane vesicles. J. Biol. Chem. **279**, 54849–54861.
128) Tonoki, A., Kuranaga, E., Tomioka, T., Hamazaki, J., Murata, S., Tanaka, K. and Miura, M. (2009) Genetic evidence linking age-dependent attenuation of the 26S proteasome with aging process. Mol. Cell Biol. (in press).
129) Tanaka, K., Yoshimura, T., Tamura, T., Fujiwara, T., Kumatori, A. and Ichihara, A. (1990) Possible mechanism of nuclear translocation of proteasomes. FEBS Lett. **271**, 41–46.
130) Ferdous, A., Kodadek, T. and Johnston, S. A. (2002) A nonproteolytic function of the 19S regulatory subunit of the 26S proteasome is required for efficient activated transcription by human RNA polymerase II. Biochemistry **41**, 12798–12805.
131) Collins, G. A. and Tansey, W. P. (2006) The proteasome: a utility tool for transcription? Curr. Opin. Genet. Dev. **16**, 197–202.
132) Russell, S. J., Reed, S. H., Huang, W., Friedberg, E. C. and Johnston, S. A. (1999) The 19S regulatory complex of the proteasome functions independently of proteolysis in nucleotide excision repair. Mol. Cell **3**, 687–695.
133) Reed, S. H. and Gillette, T. G. (2007) Nucleotide excision repair and the ubiquitin proteasome pathway–do all roads lead to Rome? DNA Repair (Amst.) **6**, 149–156.
134) Wahlman, J., DeMartino, G. N., Skach, W. R., Bulleid, N. J., Brodsky, J. L. and Johnson, A. E. (2007) Real-time fluorescence detection of ERAD substrate retrotranslocation in a mammalian *in vitro* system. Cell **129**, 943–955.
135) Tanaka, K. (1998) Proteasomes: structure and biology. J. Biochem. (Tokyo) **123**, 195–204.
136) Goldberg, A. L. (2007) Functions of the proteasome: from protein degradation and immune surveillance to cancer therapy. Biochem. Soc. Trans. **35**, 12–17.
137) Jensen, T. J., Loo, M. A., Pind, S., Williams, D. B., Goldberg, A. L. and Riordan, J. R. (1995) Multiple proteolytic systems, including the proteasome, contribute to CFTR processing. Cell

83, 129–135.
138) Meng, L., Mohan, R., Kwok, B. H., Elofsson, M., Sin, N. and Crews, C. M. (1999) Epoxomicin, a potent and selective proteasome inhibitor, exhibits in vivo antiinflammatory activity. Proc. Natl. Acad. Sci. USA **96**, 10403–10408.
139) Adams, J. (2004) The proteasome: a suitable antineoplastic target. Nat. Rev. Cancer **4**, 349–360.
140) Voorhees, P. M. and Orlowski, R. Z. (2006) The proteasome and proteasome inhibitors in cancer therapy. Annu. Rev. Pharmacol. Toxicol. **46**, 189–213.
141) Prudhomme, J., McDaniel, E., Ponts, N., Bertani, S., Fenical, W., Jensen, P. and Le Rock, K. (2008) Marine actinomycetes: a new source of compounds against the human malaria parasite. PloS One **3**, e2335.
142) Yang, H., Landis-Piwowar, K. R., Chen, D., Milacic, V. and Dou, Q. P. (2008) Natural compounds with proteasome inhibitory activity for cancer prevention and treatment. Curr. Protein Pept. Sci. **9**, 227–239.

(Received Sept. 19, 2008; accepted Nov. 28, 2008)

Profile

Keiji Tanaka was born in 1949 and started his research career in 1972 with studies on the amino acid and protein metabolism in the Institute of Enzyme Research, after graduating from the Faculty of Medicine (School of Nutrition) at The University of Tokushima. He received his Ph.D. from The University of Tokushima in 1980, working on the hepatic protein metabolism. He was promoted to assistant professor in 1976 and associate professor in 1995 at the Institute for Enzyme Research at The University of Tokushima, and head of the Department of Molecular Oncology in 1996 and Vice-Director in 2002 at The Tokyo Metropolitan Institute of Medical Science. He is an acting director at The Tokyo Metropolitan Institute of Medical Science since 2006. Over the past 25 years, he focused on elucidating the structure and molecular/physiological functions of the proteasome. The discoveries of proteasomes in 1988, immunoproteasomes in 1994, hybrid proteasomes in 2000, and thymoproteasomes in 2007 are the highlights of his study. His current research interests include intracellular proteolysis mediated by the proteasome, ubiquitin, and autophagy system in eukaryotes in general. He was awarded the Naito Memorial Foundation Prize in 2003, the Asahi Culture Prize and the Uehara Prize in 2004, and the Toray Science Technology Prize in 2007. At present he is a gust professor of Ochanomizu Woman's University, Tokyo Medical and Dental University, The University of Tokyo Graduate School of Frontier Sciences, Juntendo University School of Medicine, and Niigata University School of Medicine.

ARTICLES

nature structural & molecular biology

Crystal structure of a chaperone complex that contributes to the assembly of yeast 20S proteasomes

Hideki Yashiroda[1,10], Tsunehiro Mizushima[2,10], Kenta Okamoto[3], Tomie Kameyama[1], Hidemi Hayashi[4,5], Toshihiko Kishimoto[5,6], Shin-ichiro Niwa[4], Masanori Kasahara[7], Eiji Kurimoto[3], Eri Sakata[1,3], Kenji Takagi[2], Atsuo Suzuki[2], Yuko Hirano[1], Shigeo Murata[1,8], Koichi Kato[3,9], Takashi Yamane[2] & Keiji Tanaka[1]

Eukaryotic 20S proteasomes are composed of two α-rings and two β-rings, which form an αββα stacked structure. Here we describe a proteasome-specific chaperone complex, designated Dmp1–Dmp2, in budding yeast. Dmp1–Dmp2 directly bound to the α5 subunit to facilitate α-ring formation. In Δ*dmp1* cells, α-rings lacking α4 and decreased formation of 20S proteasomes were observed. Dmp1–Dmp2 interacted with proteasome precursors early during proteasome assembly and dissociated from the precursors before the formation of half-proteasomes. Notably, the crystallographic structures of Dmp1 and Dmp2 closely resemble that of PAC3—a mammalian proteasome-assembling chaperone; nonetheless, neither Dmp1 nor Dmp2 showed obvious sequence similarity to PAC3. The structure of the Dmp1–Dmp2–α5 complex reveals how this chaperone functions in proteasome assembly and why it dissociates from proteasome precursors before the β-rings are assembled.

© 2008 Nature Publishing Group http://www.nature.com/nsmb

The 26S proteasome is a large protein complex consisting of a catalytic core particle (the 20S proteasome) and the 19S regulatory particle[1,2]. The 20S proteasome is a cylindrical particle formed by the axial stacking of four heteroheptameric rings: two outer α-rings and two inner β-rings, each of which is made up of seven structurally similar α and β subunits, respectively, interact to create a $\alpha_{1-7}\beta_{1-7}\beta_{1-7}\alpha_{1-7}$ structure.

The molecular mechanisms underlying the assembly of 20S proteasomes have attracted a great deal of interest in recent years. The proteasome from the archaebacterium *Thermoplasma acidophilum* has a quaternary structure that is essentially identical to that of eukaryotic proteasomes, although it is composed of only two different subunits, α and β. Coexpression of these subunits in *Escherichia coli* results in complete and proteolytically active proteasomes[3]. Although deletion of the propeptide of the β subunit has no effect on proteasome assembly in *T. acidophilum*, the assembly of the 20S proteasome in eukaryotes is more complicated; five of the seven β subunits (β1, β2, β5, β6 and β7) are synthesized as precursor forms with extended polypeptide sequences at their N termini, and the propeptides of the β subunits are required for eukaryotic 20S proteasomes to assemble normally[4].

Recent evidence indicates that proteasome assembly in eukaryotes requires additional chaperone molecules. In mammals, a heterodimer of proteasome-assembling chaperones 1 and 2 (PAC1-PAC2) binds to early assembly intermediates containing a restricted subset of α subunits and promotes α-ring formation[5]. PAC1-PAC2 remains attached to the α-ring after its formation and suppresses nonproductive α-ring dimerization, thereby promoting attachment of the β subunits to the α-rings. β subunits are thought to attach to the α-rings in an orderly manner in mammals as well as in yeast; in fact, incomplete precursor complexes consisting of all seven α subunits and three β subunits (β2, β3 and β4) have been identified[6,7]. Another chaperone molecule, known as the proteasome maturation factor Ump1, associates with 15S proteasome precursors[8]. In the yeast Δ*ump1* mutant, proteasome assembly and maturation are strongly impaired. In a similar way to PAC1-PAC2, a newly identified mammalian chaperone, PAC3, was also found to bind to the α-ring and to be required for proper α-ring formation[9]. Unlike PAC1-PAC2 and Ump1, however, PAC3 dissociates before the formation of half-proteasomes, a process that is coupled with the recruitment of the β subunits and Ump1.

Whether eukaryotic cells share a common mechanism for proteasome assembly is unknown. Yeast cells express Ump1 with about 30% amino acid sequence identity with the human counterpart (also called POMP and proteassemblin)[10–12], suggesting that Ump1 is probably conserved in eukaryotes. As for the PAC proteins, it was recently

[1]Laboratory of Frontier Science, Core Technology and Research Center, Tokyo Metropolitan Institute of Medical Science, Bunkyo-ku, Tokyo 113-8613, Japan. [2]Department of Biotechnology, Graduate School of Engineering, Nagoya University, Chikusa-ku, Nagoya 464-8603, Japan. [3]Department of Structural Biology and Biomolecular Engineering, Graduate School of Pharmaceutical Sciences, Nagoya City University, 3-1 Tanabe-dori, Mizuho-ku, Nagoya 467-8603, Japan. [4]Link Genomics, Inc., Chuo-ku, Tokyo 103-0024, Japan. [5]Proteome Analysis Center and [6]Department of Biomolecular Science, Faculty of Science, Toho University, Funabashi, Chiba 274-8510, Japan. [7]Department of Pathology, Hokkaido University Graduate School of Medicine, Sapporo, Hokkaido 060-8638, Japan. [8]Laboratory of Protein Metabolism, Graduate School of Pharmaceutical Sciences, the University of Tokyo, 7-3-1 Hongo, Bunkyo-ku, Tokyo 113-0033, Japan. [9]Institute for Molecular Science, National Institutes of Natural Sciences, 5-1 Higashi-yama, Myodaiji, Okazaki 444-8787, Japan. [10]These authors contributed equally to this work. Correspondence should be addressed to K. Tanaka (tanakak@rinshoken.or.jp).

Received 20 August 2007; accepted 9 January 2008; published online 17 February 2008; doi:10.1038/nsmb.1386

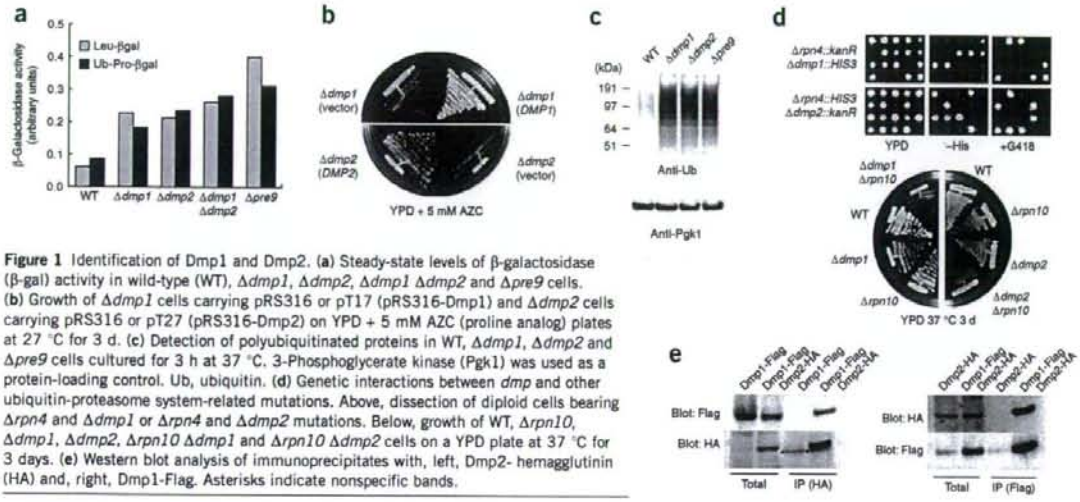

Figure 1 Identification of Dmp1 and Dmp2. (**a**) Steady-state levels of β-galactosidase (β-gal) activity in wild-type (WT), Δ*dmp1*, Δ*dmp2*, Δ*dmp1* Δ*dmp2* and Δ*pre9* cells. (**b**) Growth of Δ*dmp1* cells carrying pRS316 or pT17 (pRS316-Dmp1) and Δ*dmp2* cells carrying pRS316 or pT27 (pRS316-Dmp2) on YPD + 5 mM AZC (proline analog) plates at 27 °C for 3 d. (**c**) Detection of polyubiquitinated proteins in WT, Δ*dmp1*, Δ*dmp2* and Δ*pre9* cells cultured for 3 h at 37 °C. 3-Phosphoglycerate kinase (Pgk1) was used as a protein-loading control. Ub, ubiquitin. (**d**) Genetic interactions between *dmp* and other ubiquitin-proteasome system-related mutations. Above, dissection of diploid cells bearing Δ*rpn4* and Δ*dmp1* or Δ*rpn4* and Δ*dmp2* mutations. Below, growth of WT, Δ*rpn10*, Δ*dmp1*, Δ*dmp2*, Δ*rpn10* Δ*dmp1* and Δ*rpn10* Δ*dmp2* cells on a YPD plate at 37 °C for 3 days. (**e**) Western blot analysis of immunoprecipitates with, left, Dmp2- hemagglutinin (HA) and, right, Dmp1-Flag. Asterisks indicate nonspecific bands.

© 2008 Nature Publishing Group http://www.nature.com/nsmb

reported that in *Saccharomyces cerevisiae* Pba1 and Pba2, which show weak sequence similarity to PAC1 and PAC2, respectively, form a heterodimeric complex and bind to proteasome precursor complexes[7]. Unlike the phenotypes observed following PAC1 and PAC2 knockdowns, however, Δ*pba1* and Δ*pba2* cells show only mild defects in proteasome biogenesis.

In this paper, we describe a newly identified heterodimeric complex of Dmp1–Dmp2. Although Dmp1 and Dmp2 show no obvious sequence similarities to PAC3, the biological function and quaternary structure of this heterodimer are strikingly similar to those of PAC3. We show that Dmp1–Dmp2 is critically involved in 20S proteasome assembly, and we propose that the identified chaperone-dependent mechanisms that contribute to proteasome assembly are probably conserved among eukaryotes.

RESULTS

Isolation of *dmp* mutants

To search for genes involved in the ubiquitin-proteasome system, we streaked yeast knockout strains on YPD plates containing the proline analog L-azetidine-2-carboxylic acid (AZC; 5 mM) or SD plates containing the arginine analog canavanine (1 mg ml^{-1}) and incubated them at 26 °C for 3 d. Among the many mutants that were sensitive to the amino acid analogs, we selected 23 uncharacterized mutants on the basis of the criterion that the disrupted gene products or proteins that they interact with are conserved in higher eukaryotes. We then examined the ability of each mutant to degrade model substrates for the N-end rule pathway or the ubiquitin fusion degradation (UFD) pathway[13,14]. Because Δypl144w cells showed the most severe defect among the 23 selected mutants, we further examined the Δypl144w strain, which we named Δ*dmp1* (for degradation of misfolded proteins 1; **Fig. 1a**, **Supplementary Methods** and **Supplementary Fig. 1** online). We confirmed degradation defects in Δ*dmp1* cells by cycloheximide-chase experiments of Gcn4, a transcription activator that turns over rapidly in rich medium[15] (**Supplementary Fig. 1**). We cloned the YPL144W gene, including the 5′ and 3′ flanking regions, into the pRS316 single-copy vector. Because cloned YPL144W complemented the growth defect of the Δ*dmp1* cells on YPD + 5 mM AZC plates, we concluded that YPL144W was *DMP1* (**Fig. 1b**), which encodes a 148-residue (16.6 kDa) protein. We also confirmed that deletion of *DMP1* resulted in the stabilization of model substrates in another background strain, W303 (**Supplementary Fig. 1**).

Next we examined the accumulation of polyubiquitinated proteins in the Δ*dmp1* mutant. We used Δ*pre9* cells, which lacked the α3 subunit of the 20S proteasome, as a positive control. A larger amount of polyubiquitinated proteins accumulated in Δ*dmp1* cells than in wild-type cells, whereas the levels in Δ*dmp1* and Δ*pre9* cells were comparable (**Fig. 1c**). This result indicated that the ubiquitin-dependent degradation mediated by the 26S proteasome was impaired in Δ*dmp1* cells.

To further confirm that Dmp1 is involved in the ubiquitin-proteasome pathway, we crossed the Δ*dmp1* strain with strains carrying mutations affecting the ubiquitin-proteasome system. Rpn4 (also known as Son1 or Ufd5) is a transcriptional activator of genes encoding proteasome subunits[16,17], whereas Rpn10 (the mammalian S5a homolog) acts as a receptor capable of trapping polyubiquitinated proteins[18]. When we crossed Δ*dmp1* with Δ*rpn4*, no double mutants were obtained from 6 predicted tetratypes and 2 nonparental ditypes in tetrad analysis of 11 asci (**Fig. 1d** and data not shown). In contrast, Δ*dmp1* Δ*rpn10* double mutants were viable, but showed synthetic growth defects at high temperatures (**Fig. 1d**). These genetic interactions suggested that the ubiquitin-proteasome pathway was impaired in Δ*dmp1* cells.

Identification of Dmp1-interacting proteins

To identify proteins that interact with Dmp1, we generated a strain expressing C-terminally Flag-tagged Dmp1 from its native promoter and analyzed anti-Flag immunoprecipitates using MS. We identified three interacting proteins: one previously unknown protein encoded by YLR021W as well as the α5 (Pup2) and α6 (Pre5) subunits of the 20S proteasome (**Supplementary Fig. 2** online). Because the disruptant of the previously unknown protein displayed AZC sensitivity similar to the Δ*dmp1* strain, we named the YLR021W gene product Dmp2 (**Fig. 1b**). Dmp2 consists of 179 amino acid residues and has a molecular mass of 20.1 kDa. In addition to AZC sensitivity,

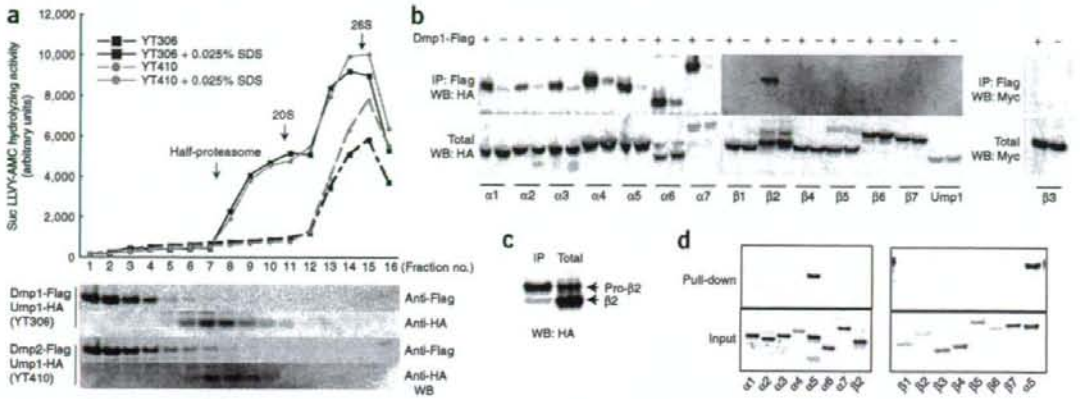

Figure 2 Characterization of the Dmp1–Dmp2 complex. (**a**) Suc-LLVY-AMC hydrolyzing activity of cell lysates fractionated by glycerol gradient centrifugation (above) and immunoblotted (WB) with anti-Flag or anti-hemagglutinin (HA) antibodies (below). The three arrows depict the locations of half-proteasomes, 20S proteasomes and 26S proteasomes. (**b**) Detection of coimmunoprecipitated (IP) proteasome subunits with Dmp1-Flag. (**c**) Comparison of the β2 subunit in the total lysate or immunoprecipitate with Dmp1-Flag. (**d**) Binding assay of recombinant GST-Dmp1–Dmp2 and the 20S proteasome subunits translated and ^{35}S-radiolabeled in reticulocyte lysates.

© 2008 Nature Publishing Group http://www.nature.com/nsmb

Δdmp2 cells showed the same phenotypes as *Δdmp1* cells, including the stabilization of model substrates and accumulation of polyubiquitinated proteins (**Fig. 1a,c**). Furthermore, we observed synthetic lethality and high temperature sensitivity when *Δdmp2* cells were crossed with *Δrpn4* and *Δrpn10* cells, respectively (**Fig. 1d**).

Next, to examine the interaction between Dmp1 and Dmp2 *in vivo*, Dmp2 was C-terminally tagged with hemagglutinin (HA). Dmp2-3×HA was immunoprecipitated from cell extracts using anti-HA antibodies. Western blots of the immunoprecipitated material using anti-Flag antibodies revealed that Dmp1-3×Flag was also present (**Fig. 1e**). Conversely, when Dmp1-3×Flag was immunoprecipitated using anti-Flag antibodies, Dmp2-3×HA was coimmunoprecipitated (**Fig. 1e**). To further confirm that Dmp1 and Dmp2 form a complex, 6×His-Dmp1 and Dmp2 were coexpressed in *E. coli* and purified using nickel-agarose beads. Dmp1 and Dmp2 formed a complex with an apparent 1:1 stoichiometry and a relative molecular mass of 43 kDa, indicating that the complex was a heterodimer (**Supplementary Fig. 3** online).

We then examined whether the *Δdmp1* phenotype was enhanced by the deletion of *DMP2*. The *Δdmp1 Δdmp2* double mutant was viable, and, compared to the single mutants, the double deletion did not enhance the stabilization of model substrates (**Fig. 1a**). This result implies that Dmp1 and Dmp2 function as a complex, and that the deletion of either protein was sufficient to eliminate the function of the heterodimeric complex.

Dmp1–Dmp2 binds to 20S proteasome precursors

To further characterize the interaction between Dmp1–Dmp2 and the proteasome subunits, cell extracts of strains expressing Ump1-HA and Dmp1-3×Flag or Dmp2-3×Flag were fractionated using 8–32% (v/v) glycerol density-gradient centrifugation. The Dmp1–Dmp2 complex and half-proteasomes containing Ump1 were detected on western blots using anti-Flag and anti-HA antibodies (**Fig. 2a**, below). Peptidase activity in each fraction was also measured to determine the distributions of the 20S and 26S proteasomes (**Fig. 2a**, above). A low concentration of SDS (0.025% (w/v)) is known to act as an artificial activator of 20S proteasomes that are usually latent in cells. This allowed us to discriminate the activity of 20S proteasomes from that of 26S proteasomes. Both Dmp1-3×Flag and Dmp2-3×Flag were primarily observed in fractions 1–4, whereas Ump1-HA was found in fractions 7–10, and 20S and 26S proteasomes were identified in fractions 10–12 and 14–15, respectively. This result indicates that the Dmp1–Dmp2 complex does not bind to the α subunits either in the half-proteasomes or in mature proteasomes.

To examine whether the Dmp1–Dmp2 complex bound specifically to α5 and α6 *in vivo*, all of the α and β subunits except β3 and Ump1 were C-terminally tagged with HA. Adding a 3×HA tag onto the C terminus of β3 caused lethality, so we constructed a strain expressing N-terminally Myc-tagged β3 under the control of the *GAL1* promoter. As shown in **Figure 2b**, when Dmp1-3×Flag was immunoprecipitated using anti-Flag M2 agarose beads, all of the α subunits were pulled down with Dmp1-3×Flag. In contrast, of the β subunits, only β2 was pulled down. Intriguingly, β2 coimmunoprecipitated as its precursor form, which was verified by comparing the coimmunoprecipitated form with β2 in the total cell lysate (**Fig. 2c**). No interaction between Ump1 and Dmp1 was detected (**Fig. 2b**). These results indicate that assembly of the 20S proteasome proceeds via a precursor complex composed of the α-ring, β2 and Dmp1–Dmp2, and that the Dmp1–Dmp2 complex dissociates from precursors before the formation of half-proteasomes containing Ump1.

We then investigated which of the proteasome subunits bind directly to Dmp1–Dmp2. Glutathione S-transferase (GST)–tagged Dmp1–Dmp2 (GST–Dmp1–Dmp2) bound to only the α5 subunit among the α and β subunits, and Ump1 translated *in vitro* (**Fig. 2d**). This result indicated that the Dmp1–Dmp2 complex bound to the proteasome precursors via direct interactions with the α5 subunit.

Impairment of 20S proteasome assembly in *Δdmp1* cells

We then examined the *Δdmp1* phenotype in more detail, focusing on proteasome biogenesis. Extracts from wild-type or *Δdmp1* cells were fractionated using 8–32% (v/v) glycerol gradient centrifugation, and the peptidase activity of each fraction was measured with or without 0.025% (w/v) SDS (**Fig. 3a**). This experiment revealed that the 20S proteasome activity was reduced by approximately 60% in *Δdmp1*

© 2008 Nature Publishing Group http://www.nature.com/nsmb

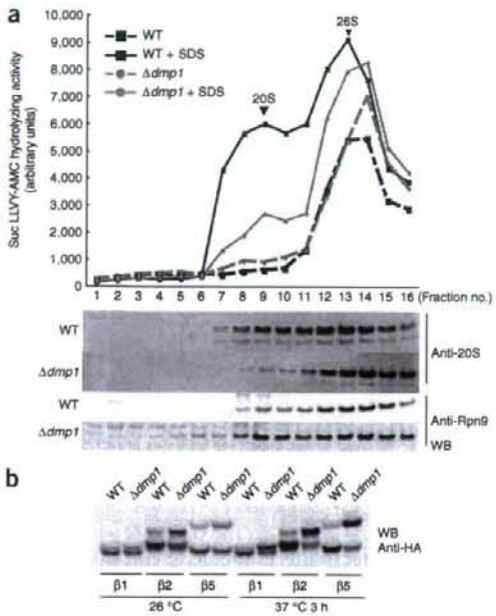

Figure 3 Impaired 20S proteasome assembly in Δ*dmp1* cells. (**a**) Suc-LLVY-AMC hydrolyzing activity of proteasomes in wild-type (WT) and Δ*dmp1* cells and immunoblotted (WB) with anti-20S (above) or anti-Rpn9 (below) antibodies. Arrowheads indicate the positions of 20S or 26S proteasomes. (**b**) WB analysis of HA-tagged β subunits in WT and Δ*dmp1* cells.

cells compared to wild-type cells. Immunoblot analysis using an antibody to yeast 20S confirmed that the level of 20S proteasome was lower in Δ*dmp1* cells (**Fig. 3a**, below). For Δ*dmp1* cells, the bands representing the 20S proteasome were faint in fractions 7–10. Conversely, the bands representing the lid component Rpn9 were slightly stronger in the fractions from Δ*dmp1* cells than in those from wild-type cells (**Fig. 3a**, below). The level of free 19S regulatory particle complexes may have increased in Δ*dmp1* cells as a result of the shortage of 20S proteasomes.

The impairment of 20S proteasome assembly in Δ*dmp1* cells was supported by the observation that the propeptides of the β subunits were not efficiently cleaved in these cells. This phenotype was more apparent at elevated temperatures (**Fig. 3b**).

Dmp1–Dmp2 is involved in α-ring formation

We further examined the involvement of the Dmp1–Dmp2 complex in proteasome biogenesis. Total cell lysates from wild-type, Δ*dmp1*, Δ*dmp2*, Δ*blm10* and Δ*pba2* cells were subjected to blue native PAGE (BN-PAGE) (**Fig. 4a**). Blm10 has been reported to be involved in a late stage of nuclear proteasome assembly and to function as a proteasome activator, although these findings remain controversial[19,20]. Pba2 has weak amino acid–sequence similarity to mammalian PAC2 (refs. 5,7). In agreement with the decreased 20S proteasome activity (**Fig. 3a**), the level of 20S proteasomes was lower in Δ*dmp1* and Δ*dmp2* cells, whereas no appreciable decrease was observed for Δ*pba2* or Δ*blm10* cells. Notably, in addition to the decrease in the level of 20S proteasomes, we observed other quickly migrating bands in the samples from Δ*dmp1* and Δ*dmp2* cells. To identify these bands, we carried out BN-PAGE and western blot analysis using strains expressing HA-tagged proteasome subunits. The results revealed that the quickly migrating bands contained all of the α subunits except α4, together with β2 (**Fig. 4b**). Tagging β6 with HA seemed to affect the assembly of the 20S proteasome, because the resulting band pattern was different from those observed from the strains expressing other tagged subunits (data not shown). Furthermore, it is noteworthy that anti-HA antibodies did not recognize the α7 subunit in mature proteasomes, whereas it clearly stained the subunit in the intermediate band, suggesting that the C-terminal portion of the α7 subunit is cleaved during maturation of the β-ring. To confirm that α4 was not part of the quickly migrating band observed in samples from Δ*dmp1* cells and to eliminate the possibility

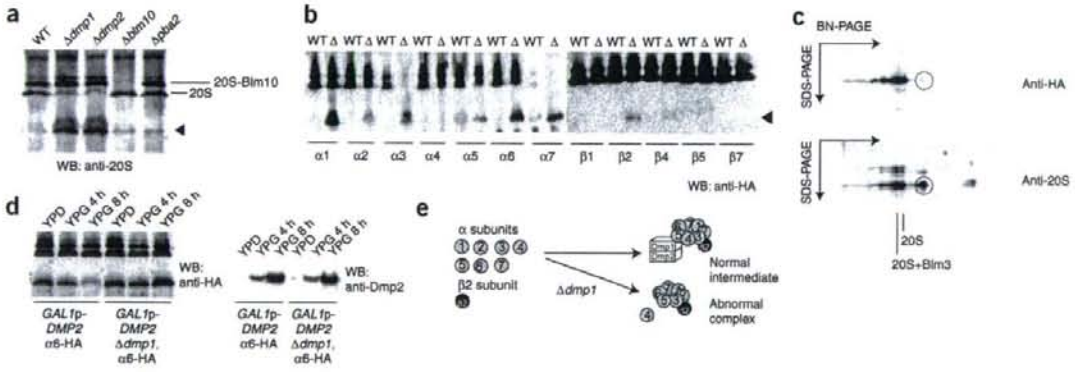

Figure 4 Detection of abnormal α-rings lacking α4 in Δ*dmp1* and Δ*dmp2* cells. Blue native (BN)-PAGE and immunoblotting (WB) with anti-20S proteasome (**a**) or anti- hemagglutinin (HA) antibodies (**b**). The filled arrowhead denotes intermediates composed of α-rings observed in Δ*dmp1* and Δ*dmp2* cells. Δ in **b** denotes Δ*dmp1*. Note in **b** that the C-terminally attached HA tag of α7 may not be present in mature proteasomes in both wild-type (WT) and Δ*dmp1* cells. (**c**) Two-dimensional BN–SDS-PAGE analysis of the proteasome in YT334 (Δ*dmp1*, α4-HA) cells. Circles denote the position of a quickly migrating band observed only in Δ*dmp1* and Δ*dmp2* cells. (**d**) Detection of abnormal complex by BN-PAGE and immunoblotting (left). Detection of Dmp2 by SDS-PAGE and immunoblotting (right). (**e**) Schematic model for Dmp1–Dmp2 function. Dmp1–Dmp2 is required for the efficient construction of the α-ring. The details of the model are provided in the text.

© 2008 Nature Publishing Group http://www.nature.com/nsmb

that the HA epitope of α4-HA was buried and inaccessible to the anti-HA antibodies, we conducted two-dimensional BN-PAGE–SDS-PAGE; the results confirmed that α4 was indeed absent from this complex (**Fig. 4c**). We then examined whether this complex was a normal intermediate or an abnormal complex using the strains in which *DMP2* is under the control of the galactose-inducible promoter. When the expression of *DMP2* was repressed in YPD medium, quickly migrating bands were observed as expected (**Fig. 4d**). If this complex is a normal intermediate, which can be detected only when the assembly step is slowed by the lack of Dmp2, it is expected to be diminished promptly when the Dmp2 proteins are supplied again. However, this complex remained even 4 h after the expression of *DMP2* was induced (**Fig. 4d**). This result suggests that the lack of Dmp1–Dmp2 results in nonproductive complexes and that the Dmp1–Dmp2 complex ensures that the steps underlying proteasome assembly occur in the proper order (**Fig. 4e**). Dmp1–Dmp2 is required for the efficient construction of α-rings and in particular for the incorporation of α4 into the α-rings.

Overall structure of the Dmp1–Dmp2 complex

To examine the structural basis of the function of this chaperone, the crystal structure of the Dmp1–Dmp2 complex was determined using multiwavelength anomalous dispersion and refined to 1.96-Å resolution (**Fig. 5a**). Dmp1 has a globular structure consisting of a six-stranded β-sheet and three α-helices. Two antiparallel sheets ($S_1$1, $S_1$2, $S_1$3 and $S_1$4, $S_1$5, $S_1$6) are composed of three β-strands joined by a parallel interaction between one strand from each sheet ($S_1$3 and $S_1$6). $H_1$1 and $H_1$3 are bound on one side of the β-sheet, and one short helix ($H_1$2) is located between $S_1$6 and $H_1$3. Dmp2, which has a globular structure similar to that of Dmp1, consists of a six-stranded β-sheet and four α-helices. Although no obvious amino acid–sequence similarity between Dmp1 and Dmp2 was observed, the tertiary structure of Dmp2 closely resembles that of Dmp1, with an average r.m.s. deviation of 3.0 Å for 103 Cα atoms (**Fig. 5a**). The loop between $S_1$4 and $S_1$5 of Dmp1 (residues 68–77), however, is distinct from the same loop in Dmp2 (residues 60–90 between $S_2$4 and $S_2$5 of Dmp2). The loop in Dmp2 is larger than that in Dmp1 and is part of a protruding structure that also contains $H_2$1 and a flexible region. The $H_2$1 helix is stabilized by a crystal contact.

The Dmp1–Dmp2 heterodimer has a β-sandwich structure formed by two six-stranded β-sheets consisting of strands $S_1$1–$S_1$6 of Dmp1 and $S_2$1–$S_2$6 of Dmp2 (**Fig. 5a,b**). This sandwich structure is surrounded by helices $H_1$1 and $H_1$3 of Dmp1 on one side and $H_2$2 and $H_2$4 of Dmp2 on the other side. Dmp1 and Dmp2 interact through an extensive interface that is approximately 25 Å long and 22 Å wide, burying a total of 2,318 Å^2 of surface area (1,159 Å^2 each for Dmp1 and Dmp2). The interface involves β-strands $S_1$1-$S_1$6, loop $S_1$2-$S_1$3 and loop $S_1$3-$S_1$4 of Dmp1, which interact against β-strands $S_2$1-$S_2$6, loop $S_2$2-$S_2$3 and loop $S_2$3-$S_2$4 of Dmp2. Dmp1–Dmp2 binding is mediated by both hydrogen bonds and van der Waals contacts (**Fig. 5c**). Residues involved in intermolecular formation of hydrogen bonds are Leu2, Pro37, Ser39, Ser53, Ser54, Leu56, Tyr59 and Leu85 of Dmp1 (located in strands $S_1$1, $S_1$3, $S_1$4 and $S_1$5, and loop $S_1$3-$S_1$4) and Glu26, Asn35, Asn36, Gln41, Arg43, Lys100 and Ser144 of Dmp2 (located in strands $S_2$2, $S_2$3, $S_2$5 and $S_2$6, and loop $S_2$2 -$S_2$3). Although the interface residues are not well conserved between Dmp1 and Dmp2, they occupy similar positions in the three-dimensional structure of each Dmp molecule (**Fig. 5d**).

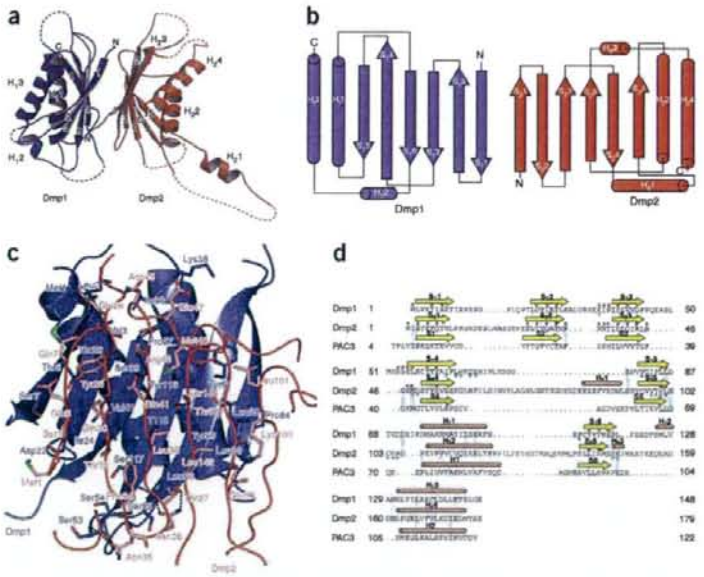

Figure 5 Structure of the Dmp1–Dmp2 complex. (**a**) A ribbon diagram of the Dmp1–Dmp2 complex. Dmp1 and Dmp2 are colored blue and red, respectively. The secondary structural elements are labeled. Dotted lines represent disordered regions. (**b**) Topology diagram of the Dmp1–Dmp2 complex. The α helices and β strands are represented by cylinders and arrows, respectively. (**c**) Close-up view of the Dmp1–Dmp2 interface showing amino acids of Dmp1 (blue) and Dmp2 (red). Hydrogen bonds are indicated by dotted lines. (**d**) Structure-based sequence alignments of Dmp1, Dmp2 and PAC3. The secondary structural elements of Dmp1, Dmp2 and PAC3 are indicated above the alignments. Identical or highly conserved residues are highlighted with a blue background. Residues that interact with Dmp2, Dmp1 and α5 are indicated by red dots, purple dots and green stars, respectively.

Structure of the Dmp1–Dmp2–α5 complex

The Dmp1–Dmp2 complex directly interacted with the α5 subunit (**Fig. 2d**). To understand the binding of Dmp1–Dmp2 to α5, we first constructed a mutant version of Dmp2 (Dmp2 Δloop), in which the protruding region (residues 61–90) was deleted to facilitate crystallization. The crystal structure of the Dmp1–Dmp2 Δloop–α5 complex was determined at 2.9-Å resolution (**Fig. 6a**, above). The structure of α5, which consists of five α-helices and ten β-strands, is essentially identical to the previously reported structure of the α5 subunit in the 20S proteasome complex; these structures have an average r.m.s. deviation of 0.79 Å for the Cα positions. The H0 helix of α5, however, is disordered in the Dmp1–Dmp2 Δloop-α5 complex (**Fig. 6a**, above). The Dmp1–Dmp2 Δloop structure in the Dmp1–Dmp2 Δloop–α5 complex can be superposed on the Dmp1–Dmp2 structure with an average r.m.s. deviation of 0.93 Å for the Cα positions, indicating that α5 binding does not cause substantial structural changes in the Dmp1–Dmp2 complex. The Dmp1–Dmp2 Δloop complex and

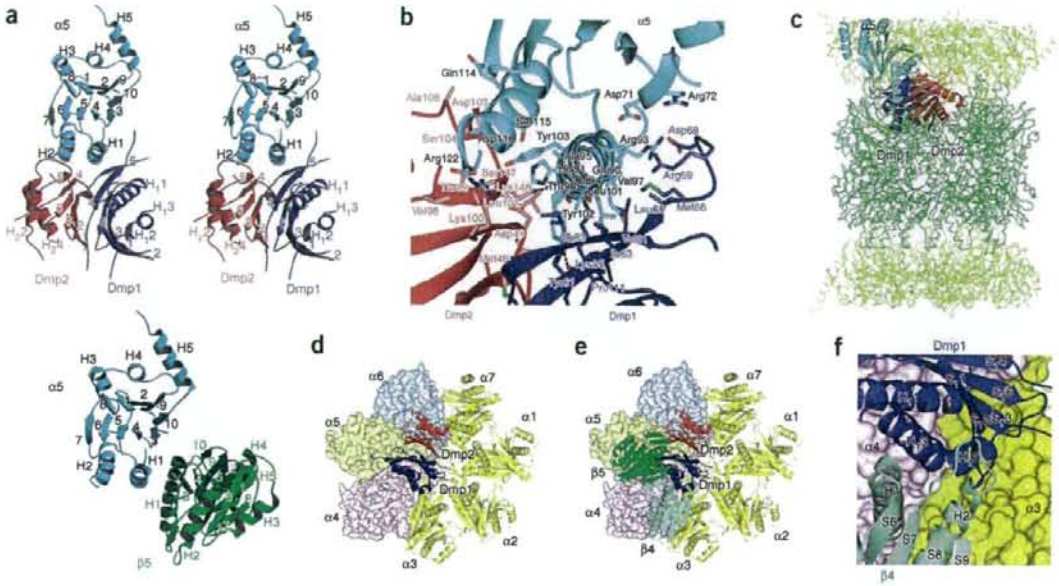

Figure 6 Structure of the Dmp1–Dmp2–α5 complex. (**a**) Above, a stereo ribbon diagram of the Dmp1–Dmp2 Δloop-α5 complex. Dmp1, Dmp2 Δloop and α5 are colored blue, red and cyan, respectively. Below, a ribbon diagram of the α5 (PDB ID code: 1RYP; chain E, cyan) and β5 (PDB ID code: 1RYP; chain L, green) complex. The secondary structural elements are labeled. (**b**) Close-up view of the Dmp1–Dmp2 Δloop–α5 interface showing amino acids of Dmp1 (blue), Dmp2 (red) and α5 (cyan). Hydrogen bonds are indicated by dotted lines. (**c**) Binding positions of the Dmp1–Dmp2 complex in the 20S proteasome. Dmp1, Dmp2 and α5 are shown as ribbon representations and are colored blue, red and cyan, respectively. Cα traces are colored yellow in the α-ring and green in the β-ring. (**d**) Model of the Dmp1–Dmp2–α-ring complex derived from the published structure of the yeast proteasome (PDB ID code: 1RYP). Dmp1, Dmp2 and the α-ring (α1, α2, α3 and α7) are shown as ribbon representations and are colored blue, red and yellow, respectively. α4 (violet), α5 (light yellow) and α6 (light blue) are shown as surface plots. (**e**) Model of the Dmp1–Dmp2–α-ring–β4–β5 complex. β4 and β5 are shown as ribbon representations and are colored light green and green, respectively. (**f**) Close-up view of the interface between Dmp1 and β4 in the model of the complex.

α5 are bound by interactions of $S_1$4, $S_1$5 and loops $S_1$2-$S_1$3, $S_1$4-$S_1$5, and $H_1$1-$S_1$6 of Dmp1; $H_2$3, $S_2$5 and loops $S_2$3-$S_2$4 and $S_2$5-$H_2$2 of Dmp2; and helices H1 and H2 of α5. The truncated loop of Dmp2 is located on the opposite side of α5. A total of 984 Å^2 of accessible surface area (557 Å^2 for Dmp1 and 427 Å^2 for Dmp2) is buried at the interface between the Dmp1–Dmp2 Δloop complex and α5. The α5 subunit binds to Dmp1–Dmp2 by packing its H1 helix against the concave surface of the Dmp1–Dmp2 complex (**Fig. 6a**, above, and **Fig. 6b**). The surface area occupied by the H1 helix of the Dmp1–Dmp2 complex is 692 Å^2. Glu90, Thr94, Val97, Leu101, Tyr102, Tyr103 and Arg122 of α5 have a central role, making multiple van der Waals contacts to Dmp1 and Dmp2. Thr94, Val97 and Tyr102 are not conserved among the α subunits of yeast proteasomes; these residues might be important for specific interactions between α5 and the Dmp1–Dmp2 complex. The intermolecular hydrogen bonds are formed by residues Tyr102, Tyr103, Asp118 and Arg122 of α5, Lys35 of Dmp1 and Met48, Thr99, Ser104, Ser147 and Lys148 of Dmp2.

The structure of the Dmp1–Dmp2 Δloop–α5 complex illustrates an intermediate state of proteasome assembly. A model of Dmp1–Dmp2 interacting with the α-ring was generated by superimposing the α5 subunit from Dmp1–Dmp2 Δloop–α5 on the structure of the 20S proteasome (PDB ID code 1RYP). In this model, Dmp1–Dmp2 bound to the inner surface of the α-ring (**Fig. 6c,d**). The Dmp1–Dmp2 binding sites in the α-ring are located more internally than those that interact with the β subunits (**Fig. 6e**). The β2, β3 and β4 subunits of the proteasomes are thought to attach to the α-rings during the primary stage of β-ring assembly. In the Dmp1–Dmp2–α-ring model, attachment of the β4 subunit to the α-ring causes steric hindrance between β4 and Dmp1 (**Fig. 6e,f**). This steric hindrance probably triggers the release of Dmp1–Dmp2 from the α-ring during the attachment of the β subunits onto the α-ring.

Structural similarity between Dmp1, Dmp2 and PAC3

The functional features of the Dmp1–Dmp2 complex discussed above are reminiscent of mammalian PAC3. PAC3 is involved in α-ring formation and is released from precursor complexes before the formation of half-proteasomes. To examine whether Dmp1–Dmp2 and PAC3 are structurally similar, we determined the crystal structure of PAC3 at 2.0-Å resolution. In the crystal, PAC3 forms a homodimer related by pseudo two-fold symmetry (**Fig. 7a**). Notably, the tertiary structure of PAC3 is strikingly similar to those of Dmp1 and Dmp2 (**Fig. 7b**). PAC3 assumes a fold composed of one six-stranded β-sheet and two α-helices: H1 and H2 (**Fig. 7c**). Superposition of PAC3 on Dmp1 and Dmp2 resulted in an average r.m.s. deviation of 3.2 Å for 107 Cα atoms and 2.0 Å for 111 Cα atoms, although no obvious sequence similarity was found even when the alignment was made on the basis of experimentally verified secondary structures (**Fig. 5d**). Comparison of the structures of Dmp1, Dmp2 and PAC3 with other known protein structures using the DALI server yielded no proteins with marked structural similarities.

© 2008 Nature Publishing Group http://www.nature.com/nsmb

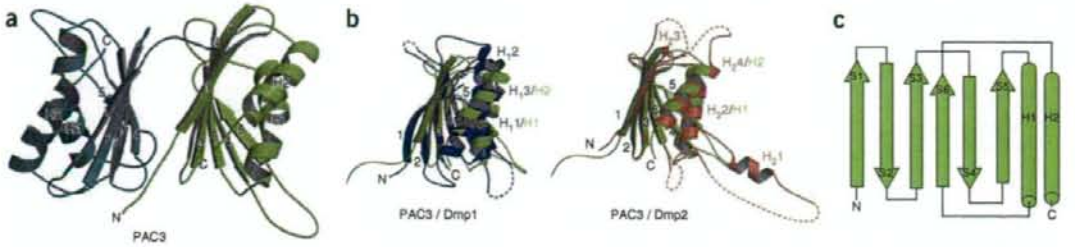

Figure 7 Structural similarity between Dmp1–Dmp2 and the human PAC3. (**a**) Structure of PAC3. A ribbon diagram of the PAC3 homodimer. Molecule A and molecule B are colored dark cyan and olive, respectively. The secondary structural elements of PAC3 are labeled. (**b**) The structure of PAC3 (olive) is compared with the structures of Dmp1 (blue) and Dmp2 (red). The secondary structural elements are labeled. (**c**) Topology diagram of PAC3. α-Helices and β-strands are represented by cylinders and arrows, respectively.

© 2008 Nature Publishing Group http://www.nature.com/nsmb

DISCUSSION

We have identified the Dmp1–Dmp2 complex as a proteasome-assembling chaperone in budding yeast. Dmp1–Dmp2 binds to proteasome subunits until they are organized into precursor complexes consisting of an α-ring and a β2 subunit and dissociates by the time the precursors become half-proteasomes, which consist of one copy of each α- and β-ring.

Whereas α-ring formation in mammals is driven by a concerted action of several chaperones (that is, the PAC1-PAC2 heterodimer and PAC3)[5,9], Dmp1 and Dmp2 are the first chaperone molecules shown to be involved in α-ring formation in yeast. Although neither Dmp1 nor Dmp2 is essential for normal growth, self-assembly of 20S proteasomes may be less efficient in the absence of Dmp1–Dmp2, particularly under stressful conditions. Supporting this idea, we detected α-rings lacking α4 in Δ*dmp1* cells but not in wild-type cells. Thus, we propose that the Dmp1–Dmp2 complex acts as a chaperone for α-ring formation (**Fig. 4e**). This complex may inhibit inappropriate binding between α3 and α5. It may also accelerate the incorporation of α4 into the α-ring. Lastly, Dmp1–Dmp2 may ensure proper β-ring assembly by masking specific docking sites on the β subunits (**Fig. 6d**) to help locate the β2 subunit at its proper position on the α-ring.

Is the function mediated by Dmp1–Dmp2 conserved in eukaryotes other than budding yeast? PAC3 shares many characteristics with Dmp1–Dmp2. In PAC3-knockdown cells, α-ring formation is impaired, leading to decreased synthesis of 20S proteasomes[9]. Disruption of Dmp1 or Dmp2 also results in decreased formation of 20S proteasomes. Unfortunately, we did not detect α-rings using glycerol gradient fractionation even in wild-type yeast cells, possibly because the assembly of the 20S proteasome occurs more rapidly in yeast than in mammals. We did, however, identify α-rings lacking α4 in Δ*dmp1* cells by BN-PAGE and western blot analysis (**Fig. 4**), indicating that, as does PAC3, Dmp1–Dmp2 has a crucial role in α-ring formation. Another feature shared by Dmp1–Dmp2 and PAC3 is that they dissociate before the formation of half-proteasomes, as is often the case with chaperone molecules.

Consistent with the functional similarities described above, X-ray structural analysis revealed that Dmp1, Dmp2 and PAC3 share extensive structural similarities. Interestingly, the overall structure of Dmp1–Dmp2 resembles those of 20S proteasome α and β subunits, although the two β-sheets in the α and β subunits are made up of five β-strands[21,22] (**Supplementary Fig. 4** online). Attachment of β5 to α5 is achieved via interactions between H1 of β5 and H1, S3 and a loop between S2 and S3 of α5 (**Fig. 6a**, below). We initially predicted that the Dmp1–Dmp2 complex would interact with α5 in a similar manner. Structural analysis, however, revealed that the binding mode of Dmp1–Dmp2 to α5 is different from that of β5 to α5 (**Fig. 6a**). In the Dmp1–Dmp2–α-ring model, Dmp1–Dmp2 is located more deeply within the α-ring, which allows Dmp1–Dmp2 to interact with α4, α5 and α6, whereas β5 interacts with only α4 and α5 (**Fig. 6e**). The unique binding mode of Dmp1–Dmp2 may be essential for its role as a proteasome-assembling chaperone.

The crystal structure of Dmp1–Dmp2–α5 also provided important insights into the molecular mechanism underlying the release of Dmp1–Dmp2 from the precursor complex. Dmp1–Dmp2 does not attach to the α-ring in the presence of β4 because of steric hindrance between β4 and Dmp1 (**Fig. 6e,f**). This model is consistent with our *in vivo* immunoprecipitation data showing that, among the β subunits, only β2 was coimmunoprecipitated with Dmp1–Dmp2 (**Fig. 2b**). Although no interaction was observed between Dmp1–Dmp2 and the β subunits *in vitro*, PAC3 directly binds to several β subunits *in vitro*. It is possible that transient and/or weak interactions with these β subunits trigger the release of PAC3 from the proteasome precursors.

In conclusion, we have demonstrated that, regardless of whether Dmp1–Dmp2 and PAC3 are evolutionarily related (**Supplementary Discussion** and **Supplementary Figs. 5** and **6** online), chaperones are likely to contribute to 20S proteasome assembly in all eukaryotes. Such mechanisms presumably became important as the 20S proteasome increased its structural complexity by acquiring seven distinct subunits for each ring.

During the preparation of this manuscript, Poc3 and Poc4 were reported to be yeast 20S proteasome assembling chaperones, which are identical to Dmp2 and Dmp1, respectively[23].

METHODS

Strains and plasmids. The *E. coli* strain DH5α was used for propagating plasmids. BL21 (DE3) cells were used for expression and purification of recombinant proteins. Strain genotypes are given in **Supplementary Table 1** online. Yeast knockout strains (catalogue number YSC1053) were purchased from Open Biosystems. The plasmids used in this study are listed in **Supplementary Table 2** online.

Immunological analysis. SDS-PAGE, BN-PAGE and western blotting were carried out with the NuPAGE system (Invitrogen) as per instructions provided by the manufacturer. Anti-Dmp2, anti-HA (Babco), anti-Flag (Sigma), anti-ubiquitin (Chemicon), anti-Pgk1 (Molecular Probe), anti-20S[24] and anti-Rpn9 (ref. 25) antibodies were used at various points during the course of this study. Anti-Dmp2 was raised in rabbits using recombinant Dmp1–Dmp2 complex. 6×His-tagged Dmp1 and Dmp2 were coexpressed in *E. coli* and purified using Ni-affinity beads.

Table 1 Data collection, phasing and refinement statistics

	Dmp1,2 (Native)	Dmp1,2 (SeMet)			Dmp1,2 Δloop–α5	PAC3 (Native)	PAC3 (SeMet)
Data collection							
Space group	$P3_1$	$P6_322$			$P2_12_12$	$P4_32_12$	$P4_32_12$
Cell dimensions							
a, *b*, *c* (Å)	57.5, 57.5, 82.2	139.1, 139.1, 92.3			158.0, 158.5, 65.2	89.1, 89.1, 57.5	86.6, 86.6, 57.2
		Peak	*Inflection*	*Remote*			
Wavelength	0.9000	0.97925	0.97945	0.96408	0.9000	1.5418	1.5418
Resolution (Å)	1.96 (2.03–1.96)		3.60 (3.73–3.60)		2.90 (3.00–2.90)	2.00 (2.07–2.00)	1.80 (1.86–1.80)
R_{merge}	0.059 (0.187)	0.093 (0.518)	0.073 (0.433)	0.105 (0.551)	0.080 (0.350)	0.084 (0.452)	0.052 (0.479)
$I / \sigma I$	24.6	12.5	13.5	11.3	20.0	14.9	15.7
Completeness (%)	98.0 (93.7)	98.8 (94.9)	84.6 (85.2)	87.2 (87.1)	99.8 (99.9)	99.9 (99.9)	99.2 (98.1)
Redundancy	4.0 (2.6)	6.1 (4.8)	4.3 (3.7)	5.3 (4.7)	6.3 (6.4)	13.2 (12.4)	12.3 (10.8)
Refinement							
Resolution (Å)	49.8–1.96				50.4–2.90	27.5–2.00	
No. reflections	20,240						
R_{work} / R_{free}	0.240 / 0.287				0.250 / 0.283	0.180 / 0.252	
No. atoms							
Protein	2,079				6,604	1883	
Water	31				0	259	
B-factors (Å^2)							
Protein	40.9				66.9	24.8	
Water	37.6					35.8	
r.m.s. deviations							
Bond lengths (Å)	0.010				0.015	0.019	
Bond angles (°)	1.393				1.757	1.663	

Values in parentheses are for highest-resolution shell. One crystal was used for each data set. SeMet, selenomethionine-substituted protein.

© 2008 Nature Publishing Group http://www.nature.com/nsmb

Protein extraction. For immunoprecipitation and protein purification, cells were suspended in lysis buffer (50 mM HEPES-KOH (pH 7.6), 100 mM β-glycerolphosphate, 50 mM NaF, 1 mM $MgCl_2$, 1 mM EGTA, 5% (v/v) glycerol and 0.25% (v/v) Triton X-100 containing complete mini EDTA-free protease inhibitors (Roche)). For glycerol gradient analysis and BN-PAGE, cells were suspended in 50 mM HEPES-KOH (pH 7.6), 1 mM $MgCl_2$, 1 mM DTT and 2 mM ATP. Total cell lysates were prepared by vortexing with glass beads using a Multibeads shocker (Yasui Kikai) and cleared by centrifugation at 20,000 × *g* for 10 min at 4 °C.

Detection of polyubiquitinated proteins. Cells were suspended in 200 ml of cold ethanol containing 2 mM PMSF. Cells were lysed by agitation with 200 ml of glass beads for 10 min. Cells lysates were dried and suspended in sample buffer for western blotting. The primary antibody was anti-ubiquitin antibody (Chemicon), and the secondary antibody was anti-mouse IgG-horseradish peroxidase (Jackson ImmunoResearch).

Coimmunoprecipitation of tagged proteins. For **Figure 2e**, cell lysates from YT145 (Dmp1-3×Flag) and YT212 (Dmp1-3×Flag and Dmp2-3×HA) cells were mixed with anti-HA antibodies and incubated for 2 h, after which protein G–Sepharose beads (GE Healthcare) were added and the mixture was incubated for 1 h (left) or cell lysates from YT211 (Dmp2-3×HA) and YT212 (Dmp1-3×Flag and Dmp2-3×HA) were mixed with anti-Flag M2 agarose beads (Sigma) and incubated for 2 h. Then, immunoprecipitates were eluted in lysis buffer containing 200 μg ml^{-1} 3×Flag peptides (Sigma; right).

Glycerol gradient analysis. Cell extracts (2 mg of protein) were separated into 32 fractions by centrifugation (22 h, 100,000 × *g*) in 8–32% (v/v) glycerol linear gradients as described previously[5].

Binding assay. *In vitro* labeling was carried out using the TNT T7 Quick for PCR DNA system (Promega) with ^{35}S-labeled methionine, according to the manufacturer's instructions. Recombinant GST–Dmp1–Dmp2 was expressed in *E. coli* and purified with glutathione-Sepharose beads. The GST–Dmp1–Dmp2–bound beads were added to the labeling mixture and incubated on ice for 1 h. The resulting products were washed with PBS containing 0.5% (v/v) Triton X-100 and eluted using 50 mM Tris-HCl (pH 8.0), 50 mM NaCl, 1 mM EDTA, 1 mM DTT and 10 mM glutathione. The eluates were separated by SDS-PAGE and visualized using autoradiography.

Assay of proteasome activity. Peptidase activity was measured using a fluorescent peptide substrate, succinyl-Leu-Leu-Val-Tyr-7-amino-4-methylcoumarin (Suc-LLVY-AMC), as described previously[5]. A low concentration of SDS (0.025% (w/v)) was used as an artificial activator of 20S proteasomes that are usually latent in cells.

Induction of Dmp2 by galactose. YT596 (*GAL1p-DMP2*, α6-HA) and YT597 (*GAL1p-DMP2*, *Δdmp1*, α6-HA) cells were grown overnight in 1.5 ml of YPD medium and then cultured in 10 ml of YPG medium to induce the expression of *DMP2* under the *GAL1* promoter. After incubation for 4 h or 8 h, cells were harvested and total cell lysates were subjected to BN-PAGE and immunoblotting with anti-HA antibodies or SDS-PAGE and immunoblotting with anti-Dmp2 antibodies.

Crystallization and data collection. Protein expression and purification were carried out as described in the **Supplementary Methods**. Crystallization of the Dmp1–Dmp2 complex was performed using the hanging-drop vapor diffusion method after mixing 3 μl of protein solution (20 mg ml^{-1}) and 1 μl of reservoir solution containing 25 mM MES (pH 6.5), 50 mM KH_2PO_4 and 16% (w/v) PEG8000. The selenomethionine (SeMet) crystals were grown at 20 °C by mixing 2 μl of protein solution and 2 μl of reservoir solution containing 0.1 M HEPES (pH 7.0) and 4.1 M NaCl. The Dmp1–Dmp2 Δloop–α5 crystals were

prepared using 0.1 M Tris-HCl (pH 8.5), 8% (v/v) ethylene glycol and 12% (w/v) PEG8000. PAC3 was crystallized using the hanging-drop vapor diffusion method after mixing 2 μl of protein solution with 2 μl of reservoir solution containing 0.1 M Tris-HCl (pH 8.5), 0.2 M $MgCl_2$ and 30% (w/v) PEG4000. SeMet PAC3 was similarly crystallized except that the pH was adjusted to 9.1.

Diffraction data sets for wild-type and SeMet Dmp1–Dmp2 as well as Dmp1–Dmp2 Δloop–α5 were collected at 100 K on beamline BL44XU (SPring-8). The diffraction data for native PAC3 and the SeMet derivative were collected using a Rigaku FR-E X-ray generator and a Rigaku R-AXIS VII detector. Data processing and reduction were carried out with the DENZO/SCALEPACK[26]. The crystal forms of wild-type Dmp1–Dmp2, SeMet Dmp1–Dmp2, Dmp1–Dmp2 Δloop–α5 and PAC3 belong to the $P3_1$, $P6_322$, $P2_12_12$, and $P4_32_12$ space groups, respectively. Data collection, phasing and refinement statistics are summarized in **Table 1**.

Structure determination and refinement. The structure of the Dmp1–Dmp2 complex was determined using multiwavelength anomalous diffraction (MAD) and SeMet proteins. The positions of heavy atoms were obtained using SHELXD[27] and refined with SHARP[28]. Initial MAD phases were extended to 3.6 Å and improved with solvent flattening and histogram mapping using DM[29]. The structure of wild-type Dmp1–Dmp2 was determined by molecular replacement using MOLREP[30] with SeMet Dmp1–Dmp2 as a search model. An initial model was built using ARP/wARP[31]. Manual building was then carried out using the program COOT[32] and alternated with several cycles of refinement using the program REFMAC5 (ref. 33).

The structure of Dmp1–Dmp2 Δloop–α5 was determined using the molecular replacement technique MOLREP and the structures of Dmp1–Dmp2 and α5 (PDB ID code 1RYP). The PAC3 structure was solved using the single-wavelength anomalous diffraction (SAD) method and the programs SHELXD and SHARP. Phasing and refinement statistics are summarized in **Table 1**. There are no residues in disallowed regions of the Ramachandran plot. Structure figures were generated using MOLSCRIPT[34], RASTER3D[35], and CCP4MG[36].

Accession codes. Protein Data Bank: Coordinates have been deposited under accession numbers 2Z5B for Dmp1–Dmp2, 2Z5C for Dmp1–Dmp2–α5 and 2Z5E for PAC3.

Note: Supplementary information is available on the Nature Structural & Molecular Biology website.

ACKNOWLEDGMENTS

We thank all of the members of BL44XU, especially E. Yamashita and M. Yoshimura, for their help in data collection at SPring-8 and T. Hikage for his help in X-ray diffraction data collection for PAC3. This work was supported by grants from Japan Science and Technology Agency (to S.M.), the Ministry of Education, Culture, Sports, Science and Technology (MEXT) of Japan (to H.Y., T.M., S.M., E.K., K.K. and K. Tanaka) and the Target Protein Project of MEXT (to T.M., K.K. and K. Tanaka and the Takeda Science Foundation (to K. Tanaka)). E.S. is a recipient of a Japan Society for the Promotion of Science Research Fellowship for Young Scientists.

AUTHOR CONTRIBUTIONS

H.Y. and T. Kameyama performed all of the yeast experiments. T.M., H.Y., K. Takagi and T.Y. determined the structures of the Dmp1–Dmp2 and Dmp1–Dmp2 Δloop–α5 complexes. K.O., E.K., E.S., A.S., Y.H., S.M., T.Y. and K.K. determined the structure of PAC3. H.H., T. Kishimoto and S.N. conducted the mass spectrometric analysis. M.K. performed phylogenetic analyses. H.Y., T.M., K.K., M.K. and K. Tanaka wrote the paper. All of the authors discussed the results and commented on the manuscript.

Published online at http://www.nature.com/nsmb/
Reprints and permissions information is available online at http://npg.nature.com/reprintsandpermissions

1. Baumeister, W., Walz, J., Zuhl, F. & Seemuller, E. The proteasome: paradigm of a self-compartmentalizing protease. *Cell* **92**, 367–380 (1998).
2. Coux, O., Tanaka, K. & Goldberg, A.L. Structure and functions of the 20S and 26S proteasomes. *Annu. Rev. Biochem.* **65**, 801–847 (1996).
3. Zwickl, P., Kleinz, J. & Baumeister, W. Critical elements in proteasome assembly. *Nat. Struct. Biol.* **1**, 765–770 (1994).
4. Chen, P. & Hochstrasser, M. Biogenesis, structure and function of the yeast 20S proteasome. *EMBO J.* **14**, 2620–2630 (1995).
5. Hirano, Y. *et al.* A heterodimeric complex that promotes the assembly of mammalian 20S proteasomes. *Nature* **437**, 1381–1385 (2005).
6. Nandi, D., Woodward, E., Ginsburg, D.B. & Monaco, J.J. Intermediates in the formation of mouse 20S proteasomes: implications for the assembly of precursor β subunits. *EMBO J.* **16**, 5363–5375 (1997).
7. Li, X., Kusmierczyk, A.R., Wong, P., Emili, A. & Hochstrasser, M. β-Subunit appendages promote 20S proteasome assembly by overcoming an Ump1-dependent checkpoint. *EMBO J.* **26**, 2339–2349 (2007).
8. Ramos, P.C., Hockendorff, J., Johnson, E.S., Varshavsky, A. & Dohmen, R.J. Ump1p is required for proper maturation of the 20S proteasome and becomes its substrate upon completion of the assembly. *Cell* **92**, 489–499 (1998).
9. Hirano, Y. *et al.* Cooperation of multiple chaperones required for the assembly of mammalian 20S proteasomes. *Mol. Cell* **24**, 977–984 (2006).
10. Burri, L. *et al.* Identification and characterization of a mammalian protein interacting with 20S proteasome precursors. *Proc. Natl. Acad. Sci. USA* **97**, 10348–10353 (2000).
11. Heink, S., Ludwig, D., Kloetzel, P.M. & Kruger, E. IFN-γ-induced immune adaptation of the proteasome system is an accelerated and transient response. *Proc. Natl. Acad. Sci. USA* **102**, 9241–9246 (2005).
12. Jayarapu, K. & Griffin, T.A. Protein-protein interactions among human 20S proteasome subunits and proteassemblin. *Biochem. Biophys. Res. Commun.* **314**, 523–528 (2004).
13. Bachmair, A., Finley, D. & Varshavsky, A. *In vivo* half-life of a protein is a function of its amino-terminal residue. *Science* **234**, 179–186 (1986).
14. Johnson, E.S., Ma, P.C., Ota, I.M. & Varshavsky, A. A proteolytic pathway that recognizes ubiquitin as a degradation signal. *J. Biol. Chem.* **270**, 17442–17456 (1995).
15. Meimoun, A. *et al.* Degradation of the transcription factor Gcn4 requires the kinase Pho85 and the SCF(CDC4) ubiquitin-ligase complex. *Mol. Biol. Cell* **11**, 915–927 (2000).
16. Mannhaupt, G., Schnall, R., Karpov, V., Vetter, I. & Feldmann, H. Rpn4p acts as a transcription factor by binding to PACE, a nonamer box found upstream of 26S proteasomal and other genes in yeast. *FEBS Lett.* **450**, 27–34 (1999).
17. Xie, Y. & Varshavsky, A. RPN4 is a ligand, substrate, and transcriptional regulator of the 26S proteasome: a negative feedback circuit. *Proc. Natl. Acad. Sci. USA* **98**, 3056–3061 (2001).
18. Glickman, M.H. *et al.* Functional analysis of the proteasome regulatory particle. *Mol. Biol. Rep.* **26**, 21–28 (1999).
19. Fehlker, M., Wendler, P., Lehmann, A. & Enenkel, C. Blm3 is part of nascent proteasomes and is involved in a late stage of nuclear proteasome assembly. *EMBO Rep.* **4**, 959–963 (2003).
20. Schmidt, M. *et al.* The HEAT repeat protein Blm10 regulates the yeast proteasome by capping the core particle. *Nat. Struct. Mol. Biol.* **12**, 294–303 (2005).
21. Groll, M. *et al.* Structure of 20S proteasome from yeast at 2.4 Å resolution. *Nature* **386**, 463–471 (1997).
22. Unno, M. *et al.* The structure of the mammalian 20S proteasome at 2.75 Å resolution. *Structure* **10**, 609–618 (2002).
23. Tallec, B. *et al.* 20S Proteasome assembly is orchestrated by two distinct pairs of chaperones in yeast and in mammals. *Mol. Cell* **27**, 660–674 (2007).
24. Tanaka, K. *et al.* Proteasomes (multi-protease complexes) as 20 S ring-shaped particles in a variety of eukaryotic cells. *J. Biol. Chem.* **263**, 16209–16217 (1988).
25. Takeuchi, J., Fujimuro, M., Yokosawa, H., Tanaka, K. & Toh-e, A. Rpn9 is required for efficient assembly of the yeast 26S proteasome. *Mol. Cell. Biol.* **19**, 6575–6584 (1999).
26. Otwinowski, Z. & Minor, W. Processing of x-ray diffraction data collected in oscillation mode. *Methods Enzymol.* **276**, 307–326 (1997).
27. Schneider, T.R. & Sheldrick, G.M. Substructure solution with SHELXD. *Acta Crystallogr. D Biol. Crystallogr.* **58**, 1772–1779 (2002).
28. Bricogne, G., Vonrhein, C., Flensburg, C., Schiltz, M. & Paciorek, W. Generation, representation and flow of phase information in structure determination: recent developments in and around SHARP 2.0. *Acta Crystallogr. D Biol. Crystallogr.* **59**, 2023–2030 (2003).
29. CCP4. The CCP4 suite: programs for protein crystallography. *Acta Crystallogr. D Biol. Crystallogr.* **50**, 760–763 (1994).
30. Vagin, A.A. & Teplyakov, A. MOLREP: an automated Program for molecular replacement. *J. Appl. Crystallogr.* **30**, 1022–1025 (1997).
31. Morris, R.J., Perrakis, A. & Lamzin, V.S. ARP/wARP and automatic interpretation of protein electron density maps. *Methods Enzymol.* **374**, 229–244 (2003).
32. Emsley, P. & Cowtan, K. Coot: model-building tools for molecular graphics. *Acta Crystallogr. D Biol. Crystallogr.* **60**, 2126–2132 (2004).
33. Murshudov, G.N., Vagin, A.A. & Dodson, E.J. Refinement of macromolecular structures by the maximum-likelihood method. *Acta Crystallogr. D Biol. Crystallogr.* **53**, 240–255 (1997).
34. Kraulis, P.J. MOLSCRIPT: a program to produce both detailed and schematic plots of protein structures. *J. Appl. Crystallogr.* **24**, 946–950 (1991).
35. Merritt, E.A. & Murphy, M.E. Raster3D Version 2.0. A program for photorealistic molecular graphics. *Acta Crystallogr. D Biol. Crystallogr.* **50**, 869–873 (1994).
36. Potterton, E., McNicholas, S., Krissinel, E., Cowtan, K. & Noble, M. The CCP4 molecular-graphics project. *Acta Crystallogr. D Biol. Crystallogr.* **58**, 1955–1957 (2002).

© 2008 Nature Publishing Group http://www.nature.com/nsmb

The EMBO Journal (2008) 27, 2204–2213 | © 2008 European Molecular Biology Organization | All Rights Reserved 0261-4189/08
www.embojournal.org

THE EMBO JOURNAL

Dissecting β-ring assembly pathway of the mammalian 20S proteasome

Yuko Hirano[1], Takeumi Kaneko[2], Kenta Okamoto[3], Minghui Bai[2], Hideki Yashiroda[2], Kaori Furuyama[2], Koichi Kato[3,4], Keiji Tanaka[1] and Shigeo Murata[2,*]

[1]Laboratory of Frontier Science, Tokyo Metropolitan Institute of Medical Science, Tokyo, Japan, [2]Laboratory of Protein Metabolism, Department of Integrated Biology, Graduate School of Pharmaceutical Sciences, The University of Tokyo, Tokyo, Japan, [3]Department of Structural Biology and Biomolecular Engineering, Graduate School of Pharmaceutical Sciences, Nagoya City University, Nagoya, Japan and [4]Division of Biomolecular Functions, Department of Life and Coordination-Complex Molecular Science, Institute for Molecular Science, National Institutes of Natural Sciences, Okazaki, Japan

The 20S proteasome is the catalytic core of the 26S proteasome. It comprises four stacked rings of seven subunits each, $\alpha_{1-7}\beta_{1-7}\beta_{1-7}\alpha_{1-7}$. Recent studies indicated that proteasome-specific chaperones and β-subunit appendages assist in the formation of α-rings and dimerization of half-proteasomes, but the process involved in the assembly of β-rings is poorly understood. Here, we clarify the mechanism of β-ring formation on α-rings by characterizing assembly intermediates accumulated in cells depleted of each β-subunit. Starting from β2, incorporation of β-subunits occurs in an orderly manner dependent on the propeptides of β2 and β5, and the C-terminal tail of β2. Unexpectedly, hUmp1, a chaperone functioning at the final assembly step, is incorporated as early as β2 and is required for the structural integrity of early assembly intermediates. We propose a model in which β-ring formation is assisted by both intramolecular and extrinsic chaperones, whose roles are partially different between yeast and mammals.

The EMBO Journal (2008) **27**, 2204–2213. doi:10.1038/emboj.2008.148; Published online 24 July 2008
Subject Categories: proteins
Keywords: assembly; chaperone; propeptide; proteasome; ubiquitin

Introduction

The ubiquitin–proteasome system is the main pathway for ATP-dependent non-lysosomal degradation of intracellular proteins in eukaryotes (Coux *et al*, 1996; Baumeister *et al*, 1998). Protein degradation achieved by this system is involved in various cellular processes, including cell cycle regulation, stress response, intracellular signalling, transcription regulation, and acquired immunity (Glickman and Ciechanover, 2002). Proteins involved in such regulatory processes as well as damaged proteins are recognized by the ubiquitin system and are marked for degradation by covalent attachment of polyubiquitin chains. Polyubiquitinated proteins are then recognized and degraded by the 26S proteasome, a 2.5-MDa multisubunit protease.

The 26S proteasome is composed of a catalytic core particle, called the 20S proteasome, bound at one or both ends by a 19S regulatory particle. The 20S proteasome is a cylindrical structure comprised of 28 subunits arranged in four stacked seven-membered rings. Each ring contains seven different subunits, whereby the two outer rings are formed by non-catalytic α-type subunits, named α1–α7, and the two inner rings are formed by the β-type subunits, β1–β7, three of which are catalytic (β1, β2, and β5) (Baumeister *et al*, 1998). Each of the 14 different proteins occupies a defined position within the 20S proteasome (Groll *et al*, 1997; Unno *et al*, 2002). Vertebrates encode four additional catalytic β-subunits; three interferon-γ-inducible β1i, β2i, and β5i and one thymus-specific β5t, which are incorporated in place of their most closely related β-subunits, thus forming distinct subtypes of proteasomes with altered catalytic activities called immunoproteasome and thymoproteasome (Tanaka and Kasahara, 1998; Murata *et al*, 2007).

The integrity of the 20S proteasome is assured by correct assembly of the 14 α-subunits and 14 β-subunits. All of the active β-subunits as well as non-catalytic β6 and β7 are synthesized with N-terminal propeptides, which are removed autocatalytically at the final step of the assembly to expose the catalytic threonine residues of β1, β2, and β5. The N-terminal active sites of β-subunits are on the inner surface of the β-rings, whereas the C termini of β-subunits are on the outer surface of the 20S proteasome (Groll *et al*, 1997). It has been shown that efficient assembly of the 20S proteasome is orchestrated by proteasome-specific chaperones such as PAC1 (Pba1 or POC1 in yeast), PAC2 (Pba2 or POC2 in yeast), PAC3 (Pba3, Dmp2, or POC3 in yeast), PAC4 (Pba4, Dmp1, or POC4 in yeast), hUmp1 (also known as POMP, proteassemblin in mammals and as Ump1 in yeast), the N-terminal propeptides of β-subunits, and C-terminal tails of β-subunits, which provide specific subunit interactions with *cis*- and *trans*-β-rings (Heinemeyer *et al*, 2004; Ramos *et al*, 2004; Hirano *et al*, 2005, 2006; Murata, 2006; Le Tallec *et al*, 2007; Li *et al*, 2007; Kusmierczyk *et al*, 2008; Yashiroda *et al*, 2008).

Proteasome assembly proceeds through distinct assembly intermediates. The earliest intermediate observed in mammalian cells is an α-ring that is comprised of all seven α-subunits, a PAC1–PAC2 heterodimer, and a PAC3–PAC4 complex (Hirano *et al*, 2005, 2006; Le Tallec *et al*, 2007). Both PAC1–PAC2 and PAC3–PAC4 are involved in the

*Corresponding author. Laboratory of Protein Metabolism, Department of Integrated Biology, Graduate School of Pharmaceutical Sciences, The University of Tokyo, 7-3-1 Hongo, Bunkyo-ku, Tokyo 113-0033, Japan. Tel.: +81 3 5841 4803; Fax: +81 3 5841 4805;
E-mail: smurata@mol.f.u-tokyo.ac.jp

Received: 14 April 2008; accepted: 3 July 2008; published online: 24 July 2008

©2008 European Molecular Biology Organization

formation of α-rings. Recently, Pba3–Pba4 or Dmp1–Dmp2, yeast orthologues of PAC3–PAC4, has shown to catalyse correct subunit orientation of an α-ring (Kusmierczyk *et al*, 2008; Yashiroda *et al*, 2008). PAC1–PAC2 prevents non-productive dimerization of α-rings. The α-ring serves as a scaffold for the assembly of β-subunits. Another intermediate is the 13S complex composed of one α-ring, unprocessed β2, β3, β4, and (h)Ump1, both in yeast and mammals (Frentzel *et al*, 1994; Nandi *et al*, 1997; Li *et al*, 2007). Recent studies in yeast showed that the addition of the other β-subunits except β7 form the subsequent intermediate referred to as a 'half-mer' precursor complex (Li *et al*, 2007; Marques *et al*, 2007). The 16S complex containing all the subunits and hUmp1 has been described also in mammalian cells (Schmidtke *et al*, 1997; Witt *et al*, 2000). A 'half-proteasome' is often used as a general term for assembly intermediates containing unprocessed β-subunits and (h)Ump1. Studies in yeast have shown that dimerization of the half-mer is driven by the propeptide of β5 and the C-terminal tail of β7, whose incorporation into the half-proteasome is coupled with the dimerization, where the role of Ump1 is proposed to be an assembly checkpoint factor that inhibits the dimerization until a full set of β-subunits are recruited on the α-ring (Ramos *et al*, 2004; Li *et al*, 2007). Removal of β-propeptides and degradation of Ump1 coincide with completion of proteasome maturation, followed by degradation of PAC1–PAC2 (Ramos *et al*, 1998; Hirano *et al*, 2005). PAC3 is released from the intermediates during the maturation process (Hirano *et al*, 2006).

Several studies in yeast reported that the propeptides and the C-terminal tails of certain β-subunits have important roles in proteasome biogenesis. The propeptide of β5 is crucial for the incorporation of β5 during proteasome formation and is thus essential for life (Chen and Hochstrasser, 1996). The propeptides of β1 and β2 are dispensable for cell viability but are known to protect the N-terminal catalytic threonine residue against N^{α}-acetylation. In addition, mutants lacking these two propeptides displayed modest defects in proteasome biogenesis (Arendt and Hochstrasser, 1999). The C-terminal tail of β2, which wraps around β3 within the same β-ring, is also essential for proteasome biogenesis in yeast (Groll *et al*, 1997; Ramos *et al*, 2004). The C-terminal tail of β7, which is inserted into a groove between β1 and β2 in the opposite ring, also has an important function in dimerization of half-proteasomes as well as stabilization of active conformation of β1 (Groll *et al*, 1997; Ramos *et al*, 2004). In mammals, analysis of propeptides has been mainly conducted in the context of immunoproteasome formation, but there is little or no information on the C-terminal tails of β2 and β7, whose location in the mammalian proteasome closely resembles those of yeast β2 and β7 in the yeast proteasome (Unno *et al*, 2002).

Here, we describe a series of biochemical experiments employing RNA interference of each β-subunit, which resulted in the accumulation of distinct assembly intermediates. By characterizing these intermediates, we clarified the order of β-subunit incorporation on the α-ring. We also assessed the roles of propeptides and C-terminal tails of β-subunits in mammalian proteasome biogenesis, which revealed that these appendages mostly function in a manner similar to yeast counterparts but also displayed some phenotypes not observed in yeast. Furthermore, we identified a novel function of hUmp1 in stabilizing assembly intermediate of proteasomes that has not been appreciated in yeast.

Results

Ordered assembly of β-subunits on α-ring

During the assembly pathway from the α-ring through the half-proteasome, each β-subunit assembles on the α-ring. To clarify the order of incorporation of β-subunits, we used the strategy of small interfering RNA (siRNA)-mediated knockdown of each β-subunit, which was expected to result in arrest of the assembly process before the incorporation of the targeted subunit and accumulation of a specific intermediate.

The total level of the different subunits as well as proteasome activity assessed by the peptide-hydrolysing activity of HEK293T cells transfected with siRNA targeting each β-subunit or hUmp1 was markedly reduced compared with those of control cells, suggesting that the biogenesis of proteasomes is severely impaired in each knockdown cell (Supplementary Figure S1). Each cell extract was resolved by native PAGE, followed by active staining or immunoblot analyses for α6- and all β-subunits (Figure 1). Immunoblot for α6 revealed accumulation of different complexes (molecular weight, 232–669 kDa) in each knockdown cell, as well as the normal α-ring in control cells, which have been shown to be a distinct assembly intermediate comprising all the seven α-subunits, PAC1–PAC2, and PAC3 (Hirano *et al*, 2006) (Figure 1A). Besides the major, fast-migrating band, a more slowly migrating minor band was observed for each knockdown cell except β2, β3, and hUmp1 knockdown (Figure 1A). Both the major and minor species did not show any peptide-hydrolysing activity, which was observed only in the complex of approximately 700-kDa, that is, 20S proteasomes (Figure 1B), indicating that they are assembly intermediates of 20S proteasomes.

Among the seven β-subunits, β2 was the first assembled on the α-ring based on the finding that β2 was detected in all the intermediates except for that in its own knockdown (Figure 1D) and the intermediate that accumulated in β2-knockdown cells did not contain any β-subunit (Figure 1C–I, lanes for β2 RNAi). The assembly of β3 followed that of β2; β3 was detected in the intermediates observed in β1-, β4-, β5-, β6-, and β7-knockdown cells, and thus the incorporation of β3 should precede these subunits (Figure 1E). This view was further confirmed by the fact that the intermediate in β3-knockdown cells contained only β2 among the β-subunits (Figure 1C–I, lanes for β3 RNAi). β3 assembly was followed by β4 incorporation, which would result in the formation of the 13S complex, comprising the α-ring plus β2, β3, and β4, as suggested by the presence of β4 in the intermediate in β1, β5, β6, and β7 knockdown (Figure 1F), consistent with the previous reports that identified the 13S complex as a distinct entity of proteasome precursors (Frentzel *et al*, 1994; Nandi *et al*, 1997; Li *et al*, 2007).

β5 was the next β-subunit incorporated into the 13S complex because β5 was detected only in the intermediates in β1-, β6-, and β7-knockdown cells (Figure 1G). The assembly of β6 followed that of β5, as evidenced by the presence of β6 in the intermediates of β1 and β7 knockdown

©2008 European Molecular Biology Organization

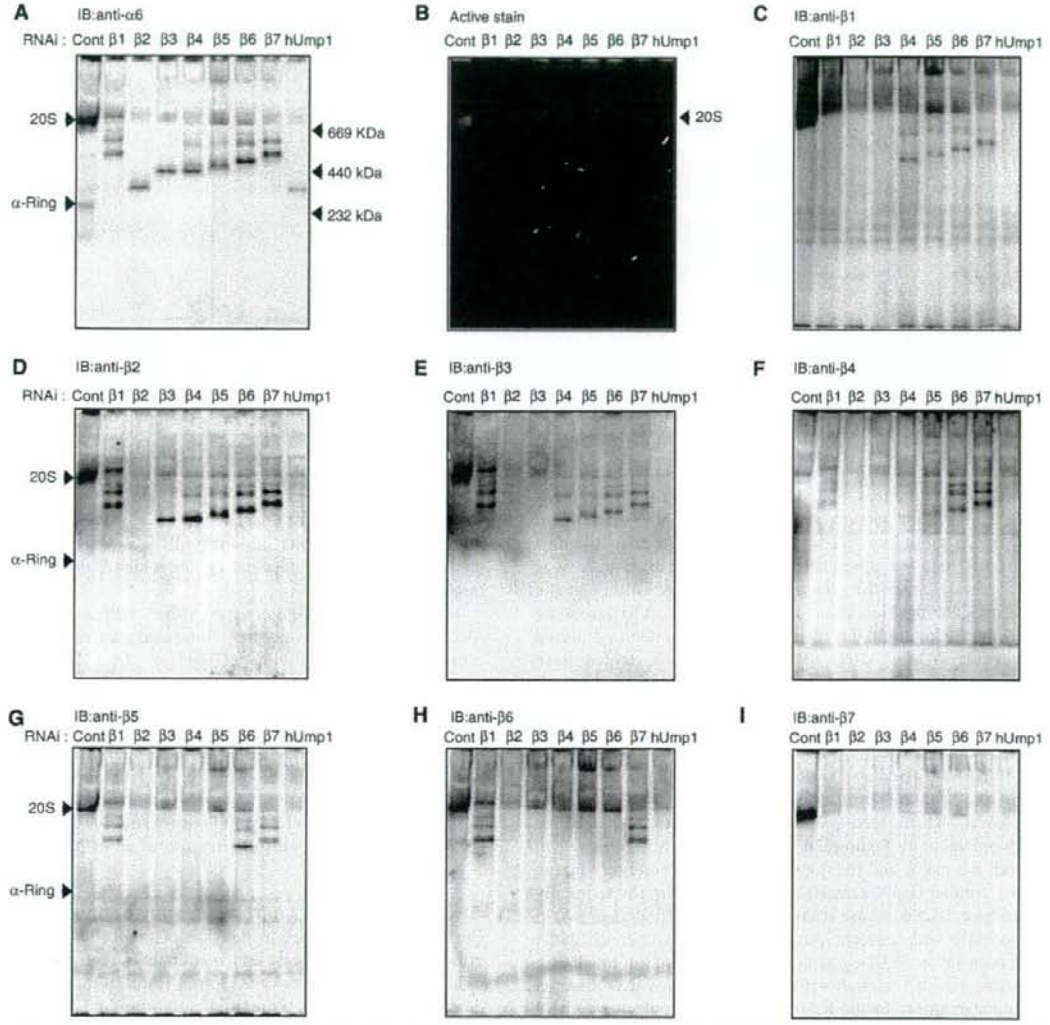

Figure 1 Accumulation of distinct assembly intermediates in each β-subunit knockdown cells. The cell extracts (40 μg) used in Supplementary Figure S1 were separated by native PAGE. Assembly intermediates were detected by immunoblotting using the indicated antibodies (**A**, **C**–**I**) The bands corresponding to α-ring and the 20S proteasome as well as the locations of molecular size markers are depicted by arrowheads. (**B**) The peptide-hydrolysing activity was assayed by active staining of the gel using Suc-LLVY-MCA in the presence of SDS. Note that the 26S proteasome did not move inside the native PAGE gel.

(Figure 1H). β7 was likely the last β-subunit incorporated in the precursor proteasomes because β7 was not found in any of the intermediate complexes (Figure 1I) and because the intermediate observed in β7-knockdown cells contained all the β-subunits with the exception of β7 (Figure 1C–I, lanes for β7 RNAi). The behaviour of β1 was rather elusive. The intermediate in β1-knockdown cells contained β2, β3, β4, β5, and β6 (Figure 1C–I, lanes for β1 RNAi), whereas β1 was already included in the intermediates of β4, β5, β6, and β7 knockdown (Figure 1C). The former observation suggests that β1 was incorporated following β2, β3, β4, β5, and β6, and that β1 is required for β7 incorporation. The latter observation suggests that the presence of β2 and β3 is sufficient for the incorporation of β1 and that β1 can be incorporated anytime during the maturation pathway from the complex containing both β2 and β3 through the half-mer.

Association of PA28, Hsp90, and Hsc70 with 20S proteasome precursors

When the same panel was probed for PAC1, the major assembly intermediate bands were associated with PAC1 (Figure 2A), which has been shown to be retained in the proteasome precursor until the completion of the assembly

©2008 European Molecular Biology Organization

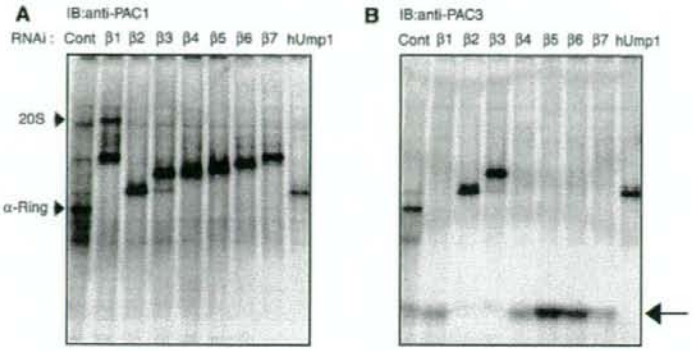

Figure 2 Release of PAC3 is coupled with β3 incorporation. The same panels in Figure 1 were probed with anti-PAC1 (**A**) and -PAC3 (**B**) antibodies. The arrow indicates PAC3 species dissociated from proteasome precursors (B).

(Hirano *et al*, 2005). However, the slowly migrating minor bands above the major bands did not contain PAC1, whereas the composition of each major and minor bands in terms of α- and β-subunits is identical (Figures 1 and 2A). It is also curious that the intermediate in β2-knockdown cells was apparently larger than the α-ring (Figure 1A), although the subunit composition is supposed to be identical to that of the α-ring. To address the identity of these bands, we tested whether PA28, PA200, Hsp90α, and Hsc70, which have been reported to be involved in proteasome biogenesis (Schmidtke *et al*, 1997; Preckel *et al*, 1999; Fehlker *et al*, 2003; Imai *et al*, 2003; Marques *et al*, 2007), associate with the intermediates.

PA28 was associated with the slow-migrating minor bands but not with the primary bands, different from PAC1 and Hsp90α, which were detected only in the major bands (Supplementary Figure S2A and B). Hsc70 was observed in both the major and the minor bands (Supplementary Figure 2C). Neither Hsp90α nor Hsc70 was detected in the α-ring. By contrast, PA200, whose yeast orthologue Blm10 was shown to associate with nascent proteasomes (Fehlker *et al*, 2003; Marques *et al*, 2007), was not observed in the intermediates, whereas its association with 20S proteasomes was detected (Supplementary Figure S2D, arrowhead). However, we cannot conclude that PA200 is not bound to assembly intermediates as free forms of PA200, which probably dissociated from 20S or nascent proteasomes during native PAGE analysis, were found (Supplementary Figure S2D, arrow).

The association of Hsp90 and Hsc70 with the assembly intermediates accounts for the increased size of the intermediate in β2-knockdown cells and suggests that recruitment of these chaperones precedes β2 and hUmp1 incorporation. The minor bands are characterized by the association of PA28, a 200-kDa heterohexameric complex. At present, we do not know whether these molecules really have some functions in the proteasome biogenesis or are associated with the intermediates as an experimental artefact. Further studies are needed to answer this question.

Release of PAC3 upon incorporation of β3

We previously showed that precursor proteasomes purified with tagged hUmp1 did not contain PAC3 and demonstrated that PAC3 is released during the maturation pathway of the mammalian proteasome (Hirano *et al*, 2006). To elucidate the step where PAC3 was released, we took advantage of the knockdown experiments in which distinct assembly intermediates accumulated depending on which β-subunit was targeted (Figure 1).

The same panel in Figure 1 was probed with anti-PAC1 and -PAC3 antibody. All the assembly intermediates as well as the α-ring were associated with PAC1 (Figure 2A) (Hirano *et al*, 2005). PAC3 is also associated with the α-ring in control cells as reported previously (Hirano *et al*, 2006). However, PAC3 was associated with intermediates of β2-, β3-, and hUmp1-knockdown cells but not with those of others, where PAC3 was found as fast migrating species, presumably as a free complex (Figure 2B, arrow). Considering the order of incorporation of β-subunits shown in Figure 1, the release of PAC3 is apparently coupled with the incorporation of β3.

A new role of hUmp1 in the assembly pathway

One intriguing difference in the phenotypes of loss of Ump1 orthologues between yeast and mammals is that knockdown of hUmp1 in mammalian cells did not result in the accumulation of intermediates containing unprocessed β-subunits (Figure 1, lanes for hUmp1 RNAi), whereas deletion of Ump1 in yeast caused apparent accumulation of such intermediates (Ramos *et al*, 1998). This observation in hUmp1-knockdown cells has also been shown in previous studies (Hirano *et al*, 2005, 2006). This finding raises the possibility that the role of Ump1 orthologues is different between yeast and mammals.

To determine the step at which hUmp1 is incorporated, the same panel in Figure 1 was probed with anti-hUmp1 antibody. hUmp1 was included in a complex other than that in β2-knockdown cells (Figure 3A), indicating that the incorporation of hUmp1 precedes that of β3. On the other hand, the intermediate in the hUmp1 knockdown complex did not contain any of the β-subunits, including β2, a finding closely resembling that in β2-knockdown cells with regard to size and composition (Figures 1 and 2; compare lanes for β2 RNAi to lanes for hUmp1 RNAi). These results suggest that incorporations of β2 and hUmp1 are coupled with each other and that loss of either result in dissociation of the other.

©2008 European Molecular Biology Organization